NASA TECHNICAL NOTE

DYNAMIC ELECTRICAL CHARACTERISTICS OF A 400-HERTZ BRAYTON CYCLE TURBOALTERNATOR AND CONTROLS

by Martin E. Valgora

Lewis Research Center
Cleveland, Ohio 44135

NATIONAL AERONAUTICS AND SPACE ADMINISTRATION • WASHINGTON, D. C. • MARCH 1971

1. Report No.	2. Government Accession No.	3. Recipient's Catalog No.
NASA TN D-6185		

4. Title and Subtitle	5. Report Date
DYNAMIC ELECTRICAL CHARACTERISTICS OF A 400-HERTZ BRAYTON CYCLE TURBOALTERNATOR AND CONTROLS	March 1971
	6. Performing Organization Code
7. Author(s)	8. Performing Organization Report No.
Martin E. Valgora	E-5956
	10. Work Unit No.
9. Performing Organization Name and Address	120-27
Lewis Research Center National Aeronautics and Space Administration Cleveland, Ohio 44135	11. Contract or Grant No.
	13. Type of Report and Period Covered
12. Sponsoring Agency Name and Address	Technical Note
National Aeronautics and Space Administration Washington, D. C. 20546	14. Sponsoring Agency Code

15. Supplementary Notes

16. Abstract

The major electrical components of a 5- to 15-kWe, 400-Hz Brayton space electric power system were operated together and found to satisfy the requirements of space application. This electrical system consists of a gas-bearing turboalternator, a voltage regulator - exciter, and a parasitic-loading speed controller. Experimental results of electrical transient tests are presented. System characteristics were determined and compared with previously obtained component test results. The following specific areas were investigated: parasitic-loading speed controller control characteristics, full-load step transients, voltage and frequency excursions and recovery times, effects of speed controller gain variation, power transients, startup and shutdown characteristics, and short-circuit performance.

17. Key Words (Suggested by Author(s))	18. Distribution Statement
Brayton cycle Turboalternator and controls Transient tests Auxiliary electric power system	Unclassified - unlimited

19. Security Classif. (of this report)	20. Security Classif. (of this page)	21. No. of Pages	22. Price*
Unclassified	Unclassified	50	$3.00

*For sale by the National Technical Information Service, Springfield, Virginia 22151

DYNAMIC ELECTRICAL CHARACTERISTICS OF A 400-HERTZ BRAYTON CYCLE TURBOALTERNATOR AND CONTROLS

by Martin E. Valgora

Lewis Research Center

SUMMARY

The major electrical components of a 5- to 15-kilowatt-electric, 400-hertz space electric power system were operated together and found to satisfy the requirements of space application.

This electrical system consists of a gas-bearing turboalternator, a voltage regulator - exciter, and a parasitic-loading speed controller. Experimental results of electrical transient tests on a system are presented. The effects of a parasitic-loading speed controller on the performance of the turboalternator and voltage regulator - exciter were determined and compared with previous results of component testing. The following specific areas were investigated: parasitic-loading speed controller control characteristics, full-load step transients, voltage and frequency excursions and recovery times, speed controller gain variation effects, power transients, startup and shutdown characteristics, and short circuit performance.

It was found that sustained speed oscillations occurred at high-gain regions of the nonlinear speed-control characteristic. By retuning the speed control, the gain was decreased and the control characteristic was linearized. After retuning, the speed response was stable and nearly critically damped. System variables recovered from all step load transients in less than a second.

The speed controller was found to decrease the maximum voltage recovery time when compared with previous results obtained without the speed controller. The electrical system was capable of automatic control during startup and shutdown tests. A low-voltage turn-on characteristic of the speed controller slowed the startup. Addition of fixed load and field current was found necessary to minimize shutdown time. No degeneration of any components or change in characteristics was found as a result of these tests.

INTRODUCTION

The NASA has been investigating systems to supply large amounts of electric power for future space missions. One very promising area of interest has been the Brayton thermodynamic cycle. This cycle uses highly efficient gas-driven turbomachinery with gas-lubricated bearings.

A 5- to 15-kilowatt-electric, two-shaft Brayton cycle power conversion system capable of providing electric power for future space missions has been investigated at Lewis. This system uses a 400-hertz gas-bearing turboalternator and a gas-bearing turbocompressor in a closed argon gas loop (ref. 1). The energy source could be a solar-collector, a nuclear reactor, or a radioisotope heater.

Gas bearings have a long lifetime and eliminate the requirement for a complex oil lubrication system and seals. The result is high reliability consistent with the 1- to 5-year mission requirement.

Space electric power system technology derived from the SNAP-8 Rankine cycle electric power system has been applied to this two-shaft Brayton cycle system. The technology in this area is currently being extended to a high-speed, single-shaft Brayton system (ref. 2).

This report describes the dynamic performance of the turboalternator, voltage regulator - exciter, and parasitic-loading speed controller operating together. These components will be referred to as the electrical system. The design parameters of this system are found in table I. These dynamic characteristics will be compared, where possible, to the previously determined component characteristics, design goals, and predictions. Specific areas of investigation in this report are (1) the frequency (speed) stability, (2) excursions in voltage and power, (3) recovery times of voltage and speed to various load changes, (4) startup and shutdown characteristics, and (5) short-circuit performance.

Previously the experimental characteristics of each electrical component were separately investigated. Results of dynamometer tests on the alternator (an electromagnetic equivalent mounted on rolling-element bearings) are found in reference 3. The voltage regulator - exciter was previously operated with this motor-driven alternator. The open-loop and closed-loop characteristics of the regulator were determined and are presented in reference 4. Steady-state and dynamic test results of the parasitic-loading speed controller tests are reported in references 5 and 6.

For this test program the turboalternator, voltage regulator - exciter, and parasitic-loading speed controller were installed in a hot-gas (argon) test facility and operated together for the first time. The test program demonstrated the feasibility of operating gas-bearing turbomachinery in a hot-gas loop. Also, effects of the voltage regulator - exciter and the parasitic-loading speed controller on the gas-bearing per-

formance were studied and found to be negligible. Results of these tests are given in references 7 to 10. In addition, the steady-state characteristics of the electrical system were also determined. They are reported in reference 11.

APPARATUS

Brayton Cycle Components

General. - The components developed under the Brayton cycle program and discussed in this report are the turboalternator, the voltage regulator - exciter, and the parasitic-loading speed controller. Reference 12 summarizes the development of these components. A schematic diagram of the experimental circuit used, including test components, is shown in figure 1.

Turboalternator. - The turboalternator (see fig. 2) consists of a two-stage axial-flow turbine that drives a four-pole homopolar inductor alternator at 12 000 rpm to generate 400-hertz electrical power. This turboalternator has gas-lubricated journal and thrust bearings and is fully described in references 7 and 8.

The liquid-cooled, radial-gap, three-phase, brushless alternator is rated at 15 kilovolt-amperes, 12 kilowatts, and 0.8 lagging power factor, at 120/208 volts. This inductor alternator has laminated pole tips containing amortisseur bars. The turboalternator output at turbine inlet design conditions is 9 kilowatts; however, in order to be conservative the alternator was designed for 12 kilowatts. In this report 9 kilowatts was used as the nominal design rating. However, the turboalternator output can be varied over a wide range by adjusting the loop gas pressure. Reference 11 found the turboalternator capable of 32 kilowatts (at unity power factor) at the maximum alternator design goal temperature. This design resulted in low losses and maximum efficiency in the 9- to 10-kilowatt output range (see ref. 3). The alternator electrical design parameters are given in table II. Additional information on the turboalternator can be found in references 9 to 11, and 13.

Voltage regulator - exciter. - The breadboard voltage regulator - exciter used for this testing is shown in figure 3. This static regulator uses both voltage and current feedback

(1) To regulate the voltage at the useful load

(2) To limit the highest phase load voltage to 132 volts

(3) To supply field current during short-circuit conditions

Details on the design and operating characteristics of this regulator are found in references 4, 11, and 13.

Parasitic-loading speed controller. - Speed regulation is achieved in this Brayton power system by adjusting the electrical load power to balance a constant turboalternator input power. The turboalternator output is absorbed by two distinct loads: the useful load (which includes all systems and equipment designated as part of an assigned mission), and the parasitic load. The parasitic load is used to compensate for variations in the useful load. Since turbine input power is fixed, a constant turboalternator load maintains speed (at approximately 12 000 rpm).

As a function of the alternator frequency, the speed controller adjusts the parasitic load by phase-controlled operation of the silicon-controlled rectifiers. A silicon-controlled rectifier controller was selected for its low shutoff (minimum parasitic load) losses. Over the operating range of the controller, parasitic load increases with increasing alternator speed. At design conditions the maximum capacity of this controller is 1.8 times the nominal turboalternator rating. This permits speed control during a possible startup condition with high turbine power (see ref. 14) or if one control section fails (off).

The controller is a breadboard construction with three separate speed-control sections. Each section is tuned to a different frequency range selected so that the characteristic of the total parasitic power against frequency is linear. Additional information on this controller may be found in references 5, 6, and 11. The speed controller (less load resistors) is shown in figure 4.

Auxiliary Equipment and Instrumentation

The useful-load bank, parasitic-load bank, contactors, switches, and wiring are standard commercial types. The useful-load bank has variable resistance and inductance, whereas the parasitic load has variable resistance only. An auxiliary direct-current power supply was used to provide field excitation current for some tests.

Because of the distorted waveforms that were encountered, all meters (see fig. 1) used were the wide-frequency-range, true-rms electronic type. Fast-responding recorder inputs for the transient tests were provided by suitable converters. Detailed information on the above instrumentation is given in tables III and IV.

Test Facility

The facility used to test the Brayton cycle components includes a motor-driven compressor to supply pressurized argon gas and an electric heater to produce rated turbine inlet temperature. In addition, the valves shown in figure 1 are provided for

turbine input power control and serve as an alternate means of controlling turboalternator speed (termed valve speed control). This facility is more fully described in references 7 and 8.

TEST PROCEDURE

In general, the electrical system was operated at its nominal design rating. At rated turbine inlet conditions the alternator output power varied from 8.8 to 9.2 kilowatts, depending on power factor. Therefore, 9 kilowatts was used as the rated useful-load output. Rated useful-load power factor was 0.8 lagging. Based on this, 9 kilowatts at 0.8 lagging power factor is 1 per unit (PU) load. The off-design condition of 0.6-lagging-power-factor useful load was also investigated.

For each useful-load power factor a parasitic power margin (minimum parasitic load) value of 320 watts was set at rated useful load. This was done by adjusting the turbine input power. This selected value was small and yet allowed good speed control throughout the tests.

Parasitic power margin is the minimum amount of parasitic power that must remain on the system in order to assure speed control when maximum useful load is stepped on. It was found in this test program and in the reference 6 tests that if the parasitic load reaches its minimum (shutoff) value as a result of the addition of useful load, the turboalternator speed will decrease and the system will shut down. For the 320-watt value determined in this report, about 170 watts were the shutoff losses and about 150 watts were the remaining controllable power to the parasitic-load resistors.

For the reference 6 tests the parasitic power margin was about 700 watts. The shutoff losses in that test were also about 170 watts. However, that testing had a higher speed controller gain and a greater frequency undershoot, which necessitated a higher power margin. Actual operation of a complete system in a flight configuration might require a different power margin.

The useful loads were removed from the electrical system in one step and reapplied in one step. These loads varied from 0 to 9 kilowatts and unity to 0.6 lagging power factor. (In this testing no leading power factor loads existed; therefore, the term lagging will henceforth be omitted.) Three-phase and single-phase short circuits were also stepped on and off the system. However, these short circuits required use of the valve speed control.

There are two modes of speed control that can be selected: (1) parasitic-loading speed control and (2) valve speed control. As shown in figure 1, the facility was equipped with a turbine bypass valve for automatic inlet pressure control and a turbine exhaust valve for pressure ratio control. The exhaust valve could be set manually, or

it could be set to automatically control speed. With the exhaust valve manually set, the turbine input power was fixed, and the turboalternator speed was controlled by the parasitic-loading speed controller. With the parasitic load inoperative, the turboalternator speed was controlled by the turbine exhaust valve. Manual control of the exhaust valve, with the parasitic-loading speed controller energized (no useful load), was used to determine the curve of parasitic power variation with frequency.

DISCUSSION OF RESULTS

Speed Controller Characteristics

Stability and gain. - Sustained oscillation occurred in the electrical system and in speed during initial testing. The instrumentation indicated power variations of 3 kilowatts and line frequency variations of 1.5 hertz. The frequency of oscillation was about 1 hertz. This stability problem was investigated by obtaining a continuous plot of total parasitic power variation with alternator frequency. This plot had to be run with a reduced parasitic-load-bank setting. This reduction in load-bank setting reduced the overall system gain and reduced the oscillations so that an acceptable plot could be obtained. The shape of this characteristic is shown in figure 5 and holds for other parasitic-load-bank settings. The total control range is from 399.8 to 406 hertz. The curve is very nonlinear and has three high-gain regions where sustained oscillations occur.

To further study the source of this problem, the characteristics of the individual speed-control sections were plotted. They were for the design parasitic-load setting (0.6 PU for each section). These plots (not shown here) had large sustained oscillations near the center of each characteristic at the same frequencies as the oscillations on the combined curve (fig. 5). This indicates that the oscillations are caused by excessive gain in each of the three individual speed-control sections and not by section overlap.

This overlap is illustrated in figure 5 by the indicated section operating ranges. Section 2 overlaps 55 percent of the section 1 range, and section 3 overlaps 73 percent of the section 2 range. Overlap is necessary to eliminate flat spots in the combined characteristic. However, excessive overlap would result in high-gain regions which could cause sustained oscillations.

The speed control was readjusted to reduce the overall gain by a factor of about 4 and to linearize the characteristic. This was accomplished by adjusting the frequency sensing circuits in each section of the speed control. This adjustment increased the operating frequency range of each section and relocated the center point of each section for satisfactory overlap. These adjustments resulted in the overall control character-

istic in figure 6. The new total control range is from 394.4 to 418.8 hertz. Note that the normal operating range is from 395.4 to 408 hertz. Since no oscillations occurred, the parasitic-load bank was reset to its design value for this curve. The curve is much smoother and has no high-gain regions.

The section operating-frequency ranges are indicated. Section 2 overlaps 38 percent of section 1, and section 3 overlaps 52 percent of section 2. Figure 6 shows that during normal operating conditions the first section and only one-half of the second are used. The remaining portion of the characteristic would be used during an overpower condition (which could occur during a startup transient (see ref. 14)), or after the failure of one of the first two sections.

The design frequency of 400 hertz now occurs near the center of the normal operating range. Previously this frequency occurred at one end of the normal operating range (see fig. 5). Moving the design frequency (speed) near the center of the normal operating range reduces the maximum frequency (speed) deviation. The normal operating frequency range is now 3.1 percent of 400 hertz, with a maximum deviation of 2.0 percent from design speed. This deviation exceeds the original design goal by 1.0 percent but was considered satisfactory for these tests. No attempt was made to obtain the minimum frequency range possible at stable system conditions.

The power factor of this control characteristic is quite nonlinear and is shown in figure 7.

The power-against-frequency characteristic (after retuning) of each speed-control section is shown in figure 8. The parasitic-load bank was adjusted to the design value on the section that was tested, with the remaining two sections set at zero parasitic load. This allowed the power variation with frequency for each individual section to be obtained. Theoretically, each section characteristic should have the same shape. However, figure 8 shows that this does not occur in practice. Each section characteristic differs noticeably from the other two. The result is a combined characteristic (fig. 6) that is nonlinear.

Figure 9 presents the incremental power gain variation of the controller as a function of parasitic power for both before and after retuning. For both curves the parasitic load is at its design value. These curves were constructed from the characteristics shown in figures 5 and 6 by taking the slope at various points. The three oscillatory regions occur at the three peaks of the upper curve in figure 9. The smallest peak is at a gain of 7.5 kilowatts per hertz. The maximum gain approached infinity and appears as a vertical section of the figure 5 curve at 404.5 hertz. After retuning. the peaks are considerably lower, with the highest peak being about one-fourth of the lowest peak before retuning. Although the overall frequency range was increased by a factor of 4 (see figs. 5 and 6), the two higher-gain peaks were reduced by much more than 4. Therefore, power gain is not inversely proportional to the frequency range.

The minimum gain values here are a function of overlap, as well as of section gain, and were reduced as expected.

The three data points indicated at 3 kilowatts on figure 9 are gain values for off-design parasitic-load settings at which sustained oscillations occurred. The upper point is an oscillatory condition before retuning. The middle point is an oscillatory condition after retuning. The lower point is the lowest gain (3.5 kW/Hz) at which oscillations occurred before retuning. The oscillation at this lower point was very small and is quite near the limit of nonoscillatory gains. These three gain values were obtained by adjusting the parasitic-load capacity above and below the design setting of 1.8 per unit. Therefore, for this speed controller, gains above 3.5 kilowatts per hertz will result in sustained oscillations and gains below this value will give the desired system stability. This gain limit (3.5 kW/Hz) is considerably less than the gain limit range of 60 to 120 kilowatts per hertz predicted to be oscillatory by the analog computer study of reference 15.

Throughout the remainder of this report "design gain" will refer to the figure 6 "after retuning" characteristic.

Failure of one speed-control section. - The parasitic-loading speed controller can continue to function after the failure (off) of any one speed-control section. Failure (off) of the first section (lowest-frequency section) will result in an upward shift in the frequency (speed) range. The new operating frequencies will range from 401 to 413 hertz for design load conditions. A failure (off) of the third section will not change the normal operating frequency range. However, the ability to control speed during an overpower condition (ref. 14) will be severely limited. This limitation is true for the failure of any section. Total parasitic power capability would be reduced from 1.8 to 1.2 per unit.

Failure (off) of the middle (second) section results in the most nonlinear characteristic. Figure 10 is a plot of this characteristic obtained by disconnecting the parasitic load of the middle speed-control section. Speed changes with load variations are quite large. The maximum speed deviation from nominal (12 000 rpm) is now 3.5 percent. In the low-gain (404 to 408 Hz) region a 0.02 per unit (approximately 0.2-kW) change results in a 4-hertz (120-rpm) change in frequency. Even though this characteristic is undesirable, it is stable and could be tolerated on a mission.

Figure 10 differs considerably from the "middle section off" characteristic previously determined in reference 6. That characteristic was determined before the speed control was retuned, and the differences in section overlap could explain the change in shape.

Shutoff losses. - In figures 5, 6, 8, and 10 the minimum value of parasitic load is the shutoff losses of the speed control. These losses do not change with the speed-control frequency range adjustment or parasitic-load-bank adjustment. Therefore, they

were found to agree with the experimental loss determination in reference 5. In figures 8 and 10 the losses are the same as in figures 5 and 6 because the individual speed-control sections (excluding the parasitic-load resistors) could not be isolated from each other (see fig. 1).

Load Step Transients

General. - The electrical system was subjected to a series of load step transients. The reduced data from these tests are found in the following sections of this report and deal with the characteristics of the voltage, power, and frequency (speed) transients.

Rated load step transients. - Rated useful load of 9 kilowatts (3 kW/phase) at 0.8 power factor was removed from and applied to the power system. The frequency transient appears in figure 11 and is seen to be stable and fast when compared with the original design goal of 1.0 second (see table V). Initially, the system was operating at rated conditions with 9 kilowatts at 0.8-power-factor useful load and minimum parasitic load (power margin). At time A the rated useful load was stepped off. Instantly the load voltage stepped up. This increase resulted from the sudden decrease in alternator-plus-line-voltage drop. Alternator power stepped down, but less than 9 kilowatts (3 kW/phase) because the remaining load, the voltage regulator - exciter (VR-E) and parasitic load, experienced the high line voltage (about 144 V). Since power is proportional to voltage squared, this remaining load was 1.44 times greater than if the voltage had not changed. Because of the increased voltage, the minimum value of alternator power at time A was fairly large (about 0.6 kW/phase). And as shown, the parasitic power stepped up slightly. At time B the voltage rapidly decreased with decreasing field current. This decay is a function of the turboalternator time constant and not dependent upon VR-E performance. This decay tends to decrease the power. However, the frequency (speed) was increasing. This turned on the speed control and tended to increase the power. These two factors tended to cancel for a short time and resulted in the small relatively flat spot in power at time B.

At time C the voltage leveled out and the speed controller continued to add load with increasing shaft speed. At time D the slope of the power curve decreased and did not match the frequency curve. This action occurred because the control characteristic was nonlinear (see fig. 6). As the speed controller turned on parasitic load, the field current increased as required to maintain constant load voltage. At time E the electrical load balanced turbine power (actually overcompensated slightly) and no further increase occurred.

The system was at steady-state value at time F and the parasitic load had changed by 3 kilowatts per phase (9 kW total), as expected. However, the alternator power was

higher than before the transient, and the field current was lower. This was caused by the increased power factor. The parasitic load at this point had a higher power factor (about 0.9) than the initial point (about 0.8). As a result there were lower alternator losses (higher output power) and less field current requirement at time F.

The useful load was applied to the system at time G, resulting in the instantaneous voltage drop (to about 101 V). This voltage drop caused the parasitic power to dip considerably (1.37 kW/phase) and limited the alternator power increase to 0.7 kilowatt per phase, rather than 3 kilowatts per phase. Because the alternator power increase at time G was small, the frequency decreased at a low rate (note frequency trace) causing a time lag (at time H) before the speed controller began to decrease power. Aided by field forcing, the VR-E rapidly raised the field current and line voltage at time H. This rise in line voltage raised the useful and parasitic power. As the alternator power reached its maximum, the voltage approached its steady-state value and the frequency decreased at a maximum rate.

The remaining transient was a function of the speed controller only. The parasitic power never recovered to its maximum value because the speed controller began to turn off before the voltage recovered. As frequency continued to decrease, the parasitic and alternator power continued to decrease until the load power balanced the turbine power. The field current decreased with alternator power and leveled off at its higher value due to the power factor decrease.

The frequency had a very slight overshoot and undershoot in this test, which indicates that the system was nearly critically damped. Although the voltage transient tends to delay the frequency transient, the system was reasonably fast and was near steady state in about 0.75 second.

Although this transient was rather typical, it differs from load step transients of other useful-load powers and power factors. Smaller useful-load-step power values reduce the magnitude of all changes. But because the voltage rises (load stepped off) act on a larger and more significant value of remaining parasitic load, the shape of the power transient changes. Also, an increase in power factor of the useful-load step reduces the magnitude of the voltage transient. This reduces the lag in speed response for loads stepped on and increases the instantaneous alternator power change. This instantaneous power change is a shock load on the bearings. These changes in magnitude and time (response) with variation in load step power and power factor are treated in more detail in following sections of this report.

The results of these tests also were compared with results of an analog computer simulation of this system (ref. 15). The simulation had a much faster power (and speed) response with some overshoot. This response results from the high gain of the simulated speed controller, about eight times the gain of the actual controller. Also the simulation had no voltage transients. Voltage transients in this test program

significantly affected the power and speed transients.

Previous test results of this speed controller coupled with an aircraft turboalternator (ref. 6) gave a frequency overshoot of 0.8 hertz and 0.6-second transient to steady-state frequency for a full load step. This report shows slight overshoot and about 0.75-second transient to steady state (fig. 11). The earlier tests were performed before the speed controller gain was reduced. This gain change would explain the increased damping and increased time response of this later testing. The difference in machine inertias was compensated for in the reference 6 tests by adjusting the aircraft turbine input power. However, that test simulating the turboalternator did not show the large sustained power oscillations that were found in this testing.

Voltage transients. - When loads are stepped on and off of an electrical system, excursions in voltage occur before the voltage regulator can correct for them. The magnitude of these excursions is primarily a function of the alternator impedance, and the recovery is a function of the VR-E and field inductance. It is desirable to minimize the magnitude and duration that the load voltage deviates from its design value. Maximum limits have been set on these two variables and are given in table V, where they are termed "maximum transient voltage" and "maximum voltage recovery time." The behavior of these variables with various useful-load steps was investigated.

Voltage excursions: Figure 12 presents voltage excursions for various useful loads stepped off and on at 1.0, 0.8, and 0.6 power factor. The family of curves is fairly linear and generally agrees with the VR-E component test results in reference 4. The differences that do exist occurred because this test was conducted under different loading conditions. In general, when a single load is applied and removed from an alternator having no other loads, the voltage rise will be larger than the dips because of the machine saturation characteristics. The reference 4 results for this alternator and VR-E show this effect. But when parasitic loads are present on a system, this relation does not necessarily hold. In reference 4 the load steps were applied and removed from the alternator and VR-E with no other loads existing. But in the tests described in this report, the useful loads were applied to the system already loaded down by the speed controller.

When the parasitic-loading speed controller was combined with the alternator - voltage regulator combination, the following factors affected the voltage excursions:

(1) Addition of the parasitic load to the useful load changed the operating region on the alternator saturation curve.

(2) For useful loads stepped off, the resulting voltage rise increased the parasitic load accordingly (V^2/R). This effect reduced the actual instantaneous load change and the resulting voltage rise.

(3) For useful loads stepped on, the voltage dip reduced the useful and parasitic loads accordingly. This effect reduced the actual instantaneous load change and the

resulting voltage dip.

The most significant result shown in figure 12 is the maximum value of the voltage rise at rated load (0.8 power factor), 24 volts. This value is less than the maximum limit specified in table V. This limit was derived from military aircraft specifications (MIL-G-6099A(ASG)). Therefore, this electrical system was found to better the typical military aircraft limits for voltage overshoot.

Voltage recovery time: Voltage recovery time is a measure of the duration of a voltage excursion and indicates how fast the voltage regulator can correct the voltage. In this report, voltage recovery time is defined as the time required for the load voltage to return to within a ±5 percent band of the final value. Ordinarily, the band is a percentage of design voltage; but, for this system, it was found that the parasitic load significantly affected the voltage regulation (see ref. 11). Therefore, in order to isolate the regulation from the recovery time, the definition stated will be used.

The voltage recovery times were found to differ from previously determined voltage recovery times without the parasitic-loading speed controller. Figure 13(a) presents voltage-recovery-time variation with increasing useful-load steps at 0.8 power factor. For loads stepped on the system, the recovery time curve is linear and agrees fairly well with the recovery results of reference 4 (reproduced in fig. 13(b)) without the speed controller. The recovery times for load stepped on are, in general, less than those for load stepped off. This relation results because VR-E field forcing occurs only on voltage dips. For loads stepped off, the recovery time curve is quite nonlinear and does not agree well with figure 13(b) results above 6 kilowatts. The previous discussion on voltage change indicated that the parasitic load imposes different load conditions on the alternator and VR-E from those in the reference 4 tests. When the results for loads stepped off are compared, it is seen that addition of the speed controller has resulted in increasing the voltage recovery time at the lowest step loads and in decreasing it at higher loads. At high useful-load-off steps, a rapid speed increase due to the large unloading occurred. This rapid speed increase adds parasitic load at a high rate, and this load increase helps restore the voltage. At low useful-load-off steps, the effect of increasing parasitic load with speed is small, but the effect of this remaining parasitic load delays the voltage recovery. When the voltage rises (low useful load stepped off), the parasitic load rises accordingly (V^2/R) and this loading minimizes the voltage rise. But then as the voltage recovers (decreases) the parasitic load decreases accordingly and tends to unload the alternator. This unloading impedes the voltage recovery (decrease) and increases the recovery time for low useful-load-off steps.

Therefore, although the parasitic-loading transient is much slower than the voltage transient, it has affected the voltage recovery. The maximum-recovery-time data occurred at a useful-load step of about 6 kilowatts and not at a full load step as normally expected.

Voltage recovery time is also a function of useful-load power factor. Lower power factors cause increased line currents and increased voltage drops, resulting in longer recovery times. Figure 14 shows variation in voltage recovery time as a function of decreasing power factor for 6-kilowatt useful-load steps. A 6-kilowatt load step, rather than 9 kilowatts, was selected for this test because it produced the highest recovery time observed in this test. Nine kilowatts is a special case when using parasitic loads. When 9 kilowatts is stepped off the electrical system, essentially no remaining load is left to be subjected to the voltage rise; whereas at all lesser values of load steps there is a significant portion of parasitic load remaining to be subjected to this voltage increase. Also electrical system load steps are ordinarily less than full load. The curves in figure 14 are linear and show an increase in recovery time with reduced power factor. At 0.6 power factor the maximum recovery time is only about 0.17 second. This value is still below the maximum limit of 0.25 second listed in table V.

In general, voltage recovery time is less for useful loads applied than for loads removed because the VR-E provides field forcing only on voltage dips.

It has been found from tests described in this section and in the preceding section that the voltage transients for the alternator and VR-E component tests do not agree with results when a parasitic-loading speed controller is added to the system.

Power transients. - When loads are stepped on and off electric power systems, power transients occur that result in shaft torque transients. In this test program it was found that large power transients are caused by large useful-load steps at high power factor. These transients can affect the performance of the gas bearings in a power system. Analytical and experimental investigations of external (launch) shock on gas bearings have been made and are presented in reference 16. The power transients discussed in this report occurred internally to the machine.

The behavior of alternator output power during a rated-useful-load step transient is shown in figure 15. The useful load was stepped off, then back on. Useful load stepped off resulted in a large step function alternator power change (dip). The alternator power then recovered to balance turbine power in an approximately exponential manner. Useful load stepped on resulted in a small step in alternator power which then increased to a maximum value and decreased exponentially. This transient approximates a half-sine pulse.

Useful-load steps with different power values and power factors were also stepped off and on the electrical system. The power fluctuations for these load steps were similar in shape (not in magnitude) to the figure 15 results. The magnitude of these transients is plotted against useful-load-step power in figure 16. Figure 16(a) presents the variation of maximum value, labeled M on figure 15, and figure 16(b) presents the variation of the instantaneous (step function) value, labeled I on figure 15. The two extremes of power factor that were run (unity and 0.6) are shown.

In both figures 16(a) and (b), the transient values are less than the steady-state value of the useful load stepped. These differences occur for the following reasons:

(1) For useful load stepped off, the voltage rise (which results from the load step, fig. 12) increases the power dissipated in the remaining (parasitic) load. This increase reduces the magnitude of the alternator power transient.

(2) For useful load stepped on, the voltage dip decreases the power of both the 9-kilowatt parasitic load already on and the added useful load. This decrease also reduces the magnitude of the alternator power transient.

(3) The maximum alternator power change is also reduced by the action of the parasitic speed controller. By the time the voltage has recovered, the speed controller has partially corrected the alternator power.

Figure 16(a) shows that the maximum value of the power change is fairly linear with load step power and does not vary much with power factor. However, figure 16(b) shows that the instantaneous value varies considerably with both load step power and power factor. This variation with power factor was further investigated.

Figure 17 shows the variation of this instantaneous value with useful-load-step power factor, with the magnitude of the useful-load step as the parameter. For a given power factor, useful load stepped off has a larger instantaneous power change than the same loads stepped on. For useful loads stepped on, the instantaneous value decreases more with power factor than for loads stepped off and is zero for all 0.6-power-factor loads. The largest instantaneous power change occurred for the 9-kilowatt, unity-power-factor useful load stepped off. It was 8.79 kilowatts (2.93 kW/phase) and was also equal to the maximum value (see fig. 16(a)).

In general, the following statements can be made relating to minimizing the effect of electrical load step transients on gas-bearing turboalternators:

(1) Several smaller load steps are preferred to one large load step.

(2) The effect of loads stepped off is greater than loads stepped on.

(3) Low-power-factor (lagging) load steps are more favorable than resistive load steps.

It is significant that no undesirable bearing performance was experienced for these Brayton components as a result of the step load tests (see ref. 7).

Frequency Transients

Frequency transients occurred with the useful-load steps previously described. These frequency transients were examined and results are presented in terms of frequency excursions and frequency recovery times.

Frequency excursions. - As shown in figure 11, the frequency does not over- or undershoot significantly. Therefore, the frequency excursions can be determined directly from the characteristic of steady-state parasitic power against frequency (fig. 6).

Frequency recovery time. - The frequency recovery time is a function of the speed controller performance, turbine input power, rotor inertia, and, to a lesser degree, the VR-E. Frequency recovery time is defined in this report as the time for the frequency to reach within 2 hertz of the final value. The 2-hertz value was selected in order to allow the voltage sufficient time to recover. Therefore, the recovery times are more representative of the speed controller response rather than of the voltage response.

The frequency recovery was found to be comparatively fast (see table V) and had very little overshoot. Because the overshoot is so small, the recovery time is actually a settling time.

Frequency-recovery-time variation with useful-load steps: Frequency-recovery-time variation with useful-load steps at 0.8 power factor is shown in figure 18. At load steps of less than 2.3 kilowatts the frequency changes less than 2 hertz, and by definition the recovery times are zero. For larger load steps, the recovery time increases but at a decreasing rate. The recovery time for load-on is longer than the recovery time for load-off for the larger load steps. This was also seen in the rated load transient (fig. 11).

The frequency recovery time is affected by the voltage recovery time. When load is applied, the instantaneous value of power change is less than when load is removed, because of the voltage dip. Therefore, the speed will change at a lower initial rate and the transient time will be lengthened. The maximum frequency recovery time is a little over 0.5 second, which is good compared to the maximum design goal of 1.0 second (see table V).

Frequency-recovery-time variation with useful-load power factor: The behavior of frequency recovery time for variable useful-load power factor is seen in figure 19 for 6-kilowatt useful-load steps. The frequency recovery time varies from about 0.36 to 0.55 second for the power factors tested. The frequency recovery time for useful loads stepped off increases slightly with reduced power factor; whereas for useful loads stepped on, the frequency recovery time increases substantially at power factors below 0.8. This increase in recovery time and the difference between the two curves results from the lag in speed response. This lag as previously discussed is caused by the decreased instantaneous power change with decreased power factor, as shown on figure 17. Again, load-on steps are, in general, longer than the load-off steps.

Frequency-recovery-time variation with speed controller gain: In order to determine the effects of speed controller gain on system performance, the number of effective speed controller sections was varied from one to three. This was accomplished by disconnecting first one, then two, parasitic-load-bank sections (see fig. 1). In each

case the total parasitic-load capacity was adjusted to slightly more than the total alternator power. This resulted in three different gains for the speed controller. One was higher, and two were lower, than in the previous tests. For this test, frequency recovery time was redefined as the time for the frequency to reach within 4 hertz of the final value, rather than the 2 hertz previously used. This change was made for two reasons: The transients were fairly long because of operation into the full-on (low gain) region of the speed-control characteristic (see fig. 6). Full-on operation can occur whenever the parasitic-load capacity is approximately equal to the turbine power. These longer transients gave the voltage additional time to recover. Also this permits a comparison with the original recovery-time design goal in table V. This goal allows 1 second to reach within 1 percent of 400 hertz (or 4 Hz).

The frequency recovery time was plotted for these gain values in figure 20 for 6-kilowatt load steps at 0.8 power factor. All gains tested resulted in recovery times of less than 1 second. Frequency recovery time decreases with increasing overall power gain, as expected. The recovery time for system design gain (three speed-control sections with 1.8 PU load capacity) was also plotted in figure 20, and this point is slightly lower than the curve. This reduced recovery time results because operation of the speed controller in the full-on region at design conditions is prevented by the parasitic overload capacity (1.8 PU).

Note that the load-stepped-off times are longer than the load-stepped-on times. This differs from previous results (figs. 18 and 19), and was also caused by operating in the full-on section of the speed-control characteristic. These recovery times would probably approach zero at about 1.0 to 1.5 kilowatts per hertz, but figure 9 showed that sustained oscillations would occur if the design gain was doubled. The maximum recovery time (to within 4 Hz of final value) experienced within design conditions was 0.38 second. It occurred for a useful-step load of 9 kilowatts at 0.8 power factor.

The effect of speed controller gain variation on the voltage recovery time was also investigated and found to be minimal. However, the higher gains did result in a more underdamped voltage behavior.

In general, the operating gain is a compromise. For this type of controller, low-frequency recovery time and good frequency regulation require high gain. But low-frequency modulation (no sustained oscillations) limits the maximum gain. In these tests the frequency recovery time and frequency regulation were not the problem - stability was. So gain was reduced at the expense of the recovery time and regulation, thus stabilizing the system.

Startup and Shutdown

The behavior of the electrical system under given startup and shutdown conditions was investigated. These tests are not typical of the startup or shutdown methods of a complete Brayton power system (see ref. 14). However, the electrical performance as a function of shaft speed (not time) is valid. The transients occurred over a relatively long duration. Therefore, the equipment and instrumentation had ample time to respond. For both startup and shutdown the electrical system automatically controlled speed (frequency) and voltage.

Startup. - Prior to rotation of the turboalternator, the facility compressor was brought up to speed. Next the facility heater was energized. Then rated turbine inlet pressure was established and the turbine exhaust valve was opened. Under these conditions the power available at the turbine was low because the facility loop was cold. Since the gas-loop warmup time was long, the startup transient occurred at essentially constant low temperature and power. The VR-E and parasitic-loading speed controller were energized during the entire startup transient.

Figure 21 shows four electrical variables and speed as a function of time. However, it is particularly pertinent that time here is not important to electrical performance. The electrical variables depend primarily on the speed of the machine.

Acceleration was slow until a stable bearing gas film was established. Residual magnetism in the alternator section of the rotor allowed voltage to build up with speed. At about 3400 rpm (25 sec) the VR-E had enough input voltage to begin supplying field current and thus further increase the voltage. The parasitic speed controller at this point was out of its voltage range and was unable to hold the parasitic load off (see ref. 5). This undesirable loading at low voltages reduced the acceleration rate. Additional loading was caused by the parasitic-load-bank autotransformers, which were saturated. (These transformers would not be present in a flight Brayton power system.) This loading effect further decreased the acceleration rate. At about 5600 rpm (49 sec), the line voltage rapidly built up to about 65 volts. This voltage is within the operating range of the speed controller and can hold the firing circuits in an off state. This allows the speed to accelerate more rapidly. Power was being supplied to the speed controller shutoff losses and the VR-E which was at high output current.

Field current increased with voltage and speed until 120 volts was reached and then it decreased as the speed increased, maintaining a constant output voltage. This voltage buildup with speed is very close to the voltage buildup test results of reference 4. At about 11 800 rpm (107 sec) the speed controller began speed regulation. This is considered to be the end of this startup, which took 107 seconds. The addition of parasitic load resulted in an increase in line current, alternator power, and field current. From this point on, the speed and voltage remained constant (in the regulation band) and the

field current varied as a function of alternator power and power factor.

Other startups were performed at higher temperatures, which resulted in higher turbine power and shorter transient times. But the performance as a function of speed did not change. The fastest startup experienced took about 12 seconds and the maximum acceleration rate for it was 1200 rpm per second, as compared with 107 seconds and 277 rpm per second maximum for the figure 21 startup.

Shutdown. - Minimizing the shutdown time of gas-bearing machinery has definite advantages. During machine deceleration, external jacking gas should be supplied to the journal and thrust bearings. The inventory of required jacking gas is proportional to shutdown time. Therefore, various methods of minimizing this shutdown time are being investigated.

Figure 22 presents for a typical shutdown the same variables shown for the startup (fig. 21). The following is the method normally used to shut down this test loop (hereinafter referred to as the normal shutdown). The facility heater was deenergized to reduce system power. All useful load was removed. The system was running at rated speed and voltage and was developing about 5 kilowatts. The VR-E was operating and all power was being dissipated by the parasitic speed controller. Time is measured from the beginning of the turbine exhaust valve closure. Manual closure of the turbine exhaust valve took about 6 seconds for this test. (The turbine bypass valve automatically opened.) During this closure the parasitic power and current both rapidly dropped off. As the speed dropped below the regulation range, the speed controller shut off. The remaining electrical power dissipation shown is VR-E losses and speed-control shutoff losses. Losses not shown include alternator losses and windage losses. The total losses reduced the speed.

Field current first reduced with decreasing parasitic power, then increased to maintain voltage as speed decreased. At about 8400 rpm (17 sec) the VR-E reached its maximum output current and then voltage began to drop rapidly with speed. The decreasing VR-E input reduced the field current (VR-E output) and therefore the voltage dropped faster than the speed. As voltage dropped off, the losses decreased and the deceleration rate decreased until the voltage reached about 42 volts. This voltage was not enough to hold the speed controller firing circuits in an off state and they turned full on (see ref. 5).

The resulting power dissipation increased the deceleration rate until the voltage regulator output ceased. At this point the deceleration rate was very low. Actually, the speed would eventually level out at a little over 2000 rpm because of leakage through the turbine exhaust valve. This valve leakage problem would not exist in a complete Brayton system. However, after the collapse of load voltage, a long coastdown time would occur. Therefore, the following method was used to stop the machine.

The alternator field was externally excited with 5 amperes from a direct-current power supply. This raised the line voltage as seen in figure 22 (at about 90 sec). Then the useful-load bank was set to 15 kilowatts (at 120 V). This loading, in addition to the parasitic load (full on), VR-E losses, and turboalternator losses, dissipated enough power to reduce the machine speed to zero within 25 seconds after the external field power was applied. The total time duration for this particular shutdown was 114 seconds. The maximum deceleration rate for this shutdown was 281 rpm per second. This normal shutdown time could have been considerably shortened by initiating the final braking action earlier. If the 15-kilowatt load (at 120 V) and the external field current were applied at about 50 seconds, the total shutdown time would have been about 75 seconds.

By changing the alternator loading conditions, much shorter shutdown times can be achieved. Figure 23 shows the speed-time characteristic for three different shutdown conditions. The upper curve (curve 1) is for the normal shutdown mode previously discussed. Application of the external braking action to stop rotation is not shown. The middle curve (curve 2) is the same as the normal shutdown (curve 1) except 12 kilowatts (at 120 V) was applied to the useful-load bank and left on throughout the shutdown. The turbine exhaust valve was rapidly closed. Here again valve leakage and voltage collapse resulted in the speed leveling off at about 3000 rpm. However, the speed reached 4000 rpm in 8.5 seconds, as compared with 47 seconds for the normal shutdown. The performance of the electrical system as a function of speed for this shutdown did not differ significantly from the normal shutdown.

If the final braking procedure, adding fixed resistance and field current, used in the normal shutdown was applied, the total shutdown would have taken place in 35 seconds. Shorter shutdown times can be accomplished by further increasing the kilowatt loading of the turboalternator and providing additional fixed field current. The shortest shutdown time is shown by curve 3. A 33-kilowatt (at 120 V) load was on the machine throughout. A constant external direct current of over 10 amperes was supplied to the field. (The VR-E was disconnected.) The valve speed-control method was substituted for the parasitic-loading method. At zero time on figure 23 the compressor motor power supply was interrupted. Now the machine reached 4000 rpm in 6 seconds and the total shutdown took place in 16 seconds. The maximum deceleration rate was 2280 rpm per second.

Shutdown time variation from 16 seconds to 114 seconds has been accomplished by controlled loading of the turboalternator. Final braking action has been found necessary to minimize the shutdown time below 4000 rpm. This would also be true if there was no valve leakage, because of the long coastdown time of the rotor. Final braking was achieved by adding fixed resistance to the machine with fixed field current. On the high-speed, single-shaft Brayton system and on future systems, this braking action will be

achieved by turning the speed controller full on and providing fixed field current.

Short Circuits

It is desirable for an electrical power system to provide enough fault current to ensure proper operation of overcurrent devices. A design goal for this system requires that the turboalternator and VR-E combination be capable of delivering three times rated alternator current to three-phase and single-phase short circuits for 5 seconds. These short circuits must be applied with the equipment hot as a result of running at rated load.

The primary purpose of this test was to determine that the equipment, and especially the gas bearings, could sustain this type of loading without performance degradation. In reference 17 analysis has indicated that high forces could be encountered if armature reaction was suddenly reduced allowing full field to be momentarily applied across the alternator air gap. However, the turboalternator test results showed that no harmful effects to the bearings or to any components could be detected.

Figure 24 shows the response of the turboalternator and VR-E to the application and removal of a three-phase (ungrounded) short circuit. The equipment was running steady-state (hot) at rated system output (9 kW at 0.8-power-factor useful load). The valve speed control was used since loss of speed control would result with the parasitic speed controller during this relatively long (5 sec) short circuit. Therefore, these two transients were not normal system performance characteristics. The transients reached steady state within 1.0 second after application and removal of the short circuit. The resulting steady-state, short-circuit current value (137 to 140 A) exceeded the 125-ampere requirement. The load current recovery after short-circuit removal was very fast and not a linear function of field current. It was concluded that this nonlinear relation results from operation of the machine in the saturation region. The maximum field current value of 12.9 amperes was the highest VR-E output recorded for all tests. The final field current value of 5.31 amperes differed from the initial rated load value of 5.00 amperes because of stator heating (increased losses) and a slight change in speed.

The single-phase (phase-to-ground) short-circuit performance is shown in figure 25. It was also applied while the system was running steady state at its rated power. The load on the two unshorted phases was not interrupted. Again the transients lasted about 1.0 second. The steady-state, short-circuit current of 210 amperes greatly exceeds the minimum goal of 125 amperes. It is significant that the steady-state phase B and phase C currents (and voltages) have decreased only 26 and 10.5 percent, respectively. The maximum field current (9.44 A) here is less than for the three-phase short circuit. This results because there is less total current feedback in the VR-E for a

single-phase short circuit than for a three-phase short circuit. The final value of 5.65 amperes also differs from the initial value for the reasons previously mentioned.

As stated, these short circuits were applied at rated system output (9 kW at 0.8-power-factor useful load). The shaft torque at this condition is 0.81 per unit alternator torque (based on 88.6 percent alternator efficiency including friction and windage, refs. 3 and 10). One per unit alternator torque occurs at rated alternator load (12 kW at 0.8 power factor) and was found in the reference 3 tests to be 7.64 lb-ft (10.35 N-m). During the three-phase short circuit the speed increased slightly, and during the single-phase short the speed decreased. This indicates the torque was less than 0.81 per unit during the three-phase short circuit and greater than 0.81 per unit during the single-phase short circuit, which agrees well with previous test results (see ref. 3).

SUMMARY OF RESULTS

The dynamic performance of the 400-hertz Brayton cycle turboalternator, voltage regulator - exciter, and parasitic-loading speed controller was experimentally investigated. The most significant results of these tests are summarized as follows:

1. Nonlinearity in the speed controller caused high-gain regions to exist in the control characteristic. These high gains caused sustained oscillations in certain regions of the operating range. To eliminate this problem, the overall gain was reduced by a factor of about 4. The gain at which sustained oscillations begin is much lower than analysis predicted.

2. The electrical system response to a rated-load (9 kW at 0.8 power factor) step removal and application was stable and nearly critically damped.

3. Voltage excursions were superior to (less than) typical military aircraft specifications (MIL-G-6099A (ASG)). The voltage and frequency recovery times were considerably less than the design goals, indicating short transient times during load changes. The voltage recovery time for this system was changed appreciably from previous results of tests without the parasitic speed controller.

4. Large useful-load steps at high power factor caused large instantaneous (step function) power changes on the alternator. These instantaneous power changes were reduced by decreasing the load step or its power factor or both.

5. The electrical system automatically controlled speed and voltage during startup and shutdown, with turbine power being fixed. Startup times varied from 12 to 107 seconds, depending on initial loop temperature. The speed controller low-voltage turnon characteristic lengthened the system startup time because of the premature parasitic loading. Shutdown times varied from 16 to 114 seconds. Power-loop shutdown time was greatly reduced by adding a fixed electrical load to the turboalternator and

providing a fixed field current. This shutdown time reduction will also reduce the bearing-jacking-gas inventory.

6. Single-phase and three-phase short circuits were applied to the turboalternator and voltage regulator - exciter while they were operating at rated power. The parasitic-loading speed controller was disconnected during these tests. Current values of 140 amperes for the three-phase short circuit and 210 amperes for the single-phase short circuit were experienced during the 5-second tests and exceeded the 125-ampere minimum requirement for each. The transients reached steady-state within 1.0 second after application or removal of the short circuits.

7. No degradation of any components, including the gas bearings, or change in any characteristic was found to have resulted from this testing.

CONCLUSIONS

Based on the results of this testing, the following conclusions were reached:

1. If the control characteristic of parasitic-loading speed controllers can be better linearized, higher average gains can be used to shorten the frequency recovery time.

2. If an operating space electric power system is experiencing problems which can affect the gas bearings, useful-load steps at reduced lagging power factor are preferred over high-power-factor steps for a given power level.

3. Turboalternator gas bearings can survive severe electrical transients.

Lewis Research Center,
National Aeronautics and Space Administration,
Cleveland, Ohio, October 21, 1970,
120-27.

REFERENCES

1. Bernatowicz, Daniel T.: NASA Solar Brayton Cycle Studies. Presented at the Symposium on Solar Dynamic Systems, Solar and Mechanical Working Groups of the Interagency Advanced Power Group, Washington, D. C., Sept. 1963.

2. Klann, John L.: 2 to 10 Kilowatt Solar or Radioisotope Brayton Power System. Intersociety Energy Conversion Engineering Conference. Vol. 1. IEEE, 1968, pp. 407-415.

3. Edkin, Richard A.; Valgora, Martin E.; and Perz, Dennis A.: Performance Characteristics of 15 KVA Homopolar Inductor Alternator for 400 Hz Brayton-Cycle Space-Power System. NASA TN D-4698, 1968.

4. Bollenbacher, Gary; Edkin, Richard A.; and Perz, Dennis A.: Experimental Evaluation of a Voltage Regulator-Exciter for a 15 Kilovolt-Ampere Brayton Cycle Alternator. NASA TN D-4697, 1968.

5. Word, John L.; Fischer, Raymond L. E.; and Ingle, Bill D.: Static Parasitic Speed Controller for Brayton-Cycle Turboalternator. NASA TN D-4176, 1967.

6. Fischer, Raymond L. E.; and Droba, Darryl J.: Dynamic Characteristics of Parasitic-Loading Speed Controller for 10-Kilowatt Brayton Cycle Turboalternator. NASA TM X-1456, 1968.

7. Wood, James C.; Valgora, Martin E.; Kruchowy, Roman; Curreri, Joseph S.; Perz, Dennis A.; and Tryon, Henry B.: Preliminary Performance Characteristics of a Gas-Bearing Turboalternator. NASA TM X-1820, 1969.

8. Wood, James C.; Valgora, Martin E.; and Tryon, Henry B.: Hot Performance Characteristics of a Gas Bearing Brayton Cycle Turboalternator. Intersociety Energy Conversion Engineering Conference. AIChE, 1969, pp. 659-667.

9. Kruchowy, Roman; Wood, James C.; and Curreri, Joseph S.: Performance of a Turboalternator Gas-Bearing System at Steady-State Conditions. NASA TN D-5542, 1969.

10. Curreri, Joseph S.; Kruchowy, Roman; and Wood, James C.: Turbine Performance in a Gas-Bearing Brayton Cycle Turboalternator. NASA TN D-5604, 1969.

11. Valgora, Martin E.; and Perz, Dennis A.: Steady-State Electrical Performance of a 400-Hertz Brayton Cycle Turboalternator and Controls. NASA TN D-5658, 1970.

12. Corcoran, Charles S.; and Yeager, Leroy J.: Summary of Electrical Component Development for a 400-Hertz Brayton Energy Conversion System. NASA TN D-4874, 1968.

13. Dryer, A. M.; Kirkpatrick, F. M.; Russell, E. F.; Wimsatt, J. M.; and Yeager, L. J.: Alternator and Voltage Regulator-Exciter for a Brayton Cycle Space Power System. Vol. 1 - Alternator and Voltage Regulator-Exciter Design and Development. NASA CR-1451, 1970.

14. Hurrell, Herbert G.; and Thomas, Ronald L.: Control and Startup Considerations for Two-Spool Solar-Brayton Power System. NASA TM X-1270, 1966.

15. Tew, Roy C.; Gerchman, Robert D.; and Hurrell, Herbert G.: Analog-Computer Study of Parasitic-Load Speed Control for Solar-Brayton System Turboalternator. NASA TN D-3784, 1967.

16. Spencer, Paul R.; Curren, Peter W.; and Tryon, Henry B.: Effects of Vibration and Shock on the Performance of Gas-Bearing Space-Power Brayton Cycle Turbomachinery. Part I - Half-Sine Shock and Sinusoidal Vibration. NASA CR-1762, 1971.

17. Greenwell, J. E.; Russell, E. F.; and Yeager, L. J.: Alternator and Voltage Regulator - Exciter for a Brayton Cycle Space Power System. Vol. 2 - Unbalanced Electromagnetic Forces Investigation. Rep. GE-A69-003, General Electric Co., May 1969.

TABLE I. - 400-HERTZ BRAYTON CYCLE ELECTRICAL SYSTEM DESIGN PARAMETERS

Rated voltage, V, rms:	
Line to neutral	120
Line to line	208
Rated frequency, Hz	400
Number of phases	3
Output power, kW	9
Maximum parasitic load power, per unit	1.8
Rated power factor, lagging	0.8

TABLE II. - ALTERNATOR DESIGN PARAMETERS

Rated voltage, V, rms:	
Line to neutral	120
Line to line	208
Rated speed, rpm	12 000
Rated frequency, Hz	400
Rated kilovolt-amperes, kVA	15
Rated power, kW	12
Rated current, A	41.7
Number of phases	3
Rated power factor, lagging	0.8
Maximum hot-spot temperature, ^{o}C	180

TABLE III. - METER SPECIFICATIONS

True rms-to-dc converter (voltage and current):	
Input rms voltage, V	0.009 to 1000
Accuracy, percent of full-scale deflection (20^{o} to 30^{o} C)	0.1
Frequency response, Hz	40 to 30×10^{3}
Input impedance paralleled with 60 to 80 pF (depending on input range), MΩ	1
Output full-scale dc voltage (depending on input range), V	3 or 10
Integrating digital voltmeter (voltage, current, and power):	
Input dc voltage, V	0 to 1000
Accuracy, percent ±1 digit	0.01
Input impedance (depending on range), MΩ	0.1 to 10
Precision shunt (current):	
Resistance, Ω	0.1
Capacity, A	15
Accuracy (in air), percent	0.04
Current transformer (current and power):	
Current ratio	100/50 to 5
Ratio error (70 to 2500 Hz), percent	±0.1
Capacity, VA	25
Wattmeter (power):	
Input voltage (nominal), V	50, 100, 200
Input current (nominal), A	5
Accuracy (output), percent	0.1
Frequency range, Hz	0 to 2500
Five-digit frequency counter (frequency and speed):	
Range, MHz	0.000002 to 2.5
Accuracy, counts in range used	±1

TABLE IV. - TRANSDUCER SPECIFICATIONS

Frequency converter (speed):	
Input voltage, V	0.01 to 5.0
Frequency range, Hz	0 to 500
Accuracy, percent	±1.0
Time constant, sec	0.125
Frequency converter (speed) expanded range:	
Input voltage, V	30 to 125
Frequency range, Hz	375 to 425
Output dc voltage, V	12 to 25
Power converter:	
Input voltage, V	0 to 140
Input current, A	0 to 5
Accuracy, percent	±2.0
Frequency range, Hz	50 to 500
Response to 99 percent of final value, sec	0.1
Voltage converter:	
Input voltage, V	0 to 150
Accuracy, percent	±1.0
Response to 99 percent of final value	0.1
Output dc voltage, V	0 to 10

TABLE V. - ELECTRICAL SYSTEM PERFORMANCE (WITHIN RATED CONDITIONS)

	Desired	Actual
Normal operating frequency range, Hz	400 to 404	395.4 to 408.0
Maximum transient voltage, V	156.9	144
Transient frequency range, Hz ± percent	400±2.0	401.7±1.57
Maximum frequency recovery time, sec	[a]1.0	[b]0.38
Maximum voltage recovery time, sec	[c]0.25	[d]0.10
Nominal turboalternator rated power output[e], kW	---------	9

[a]To within ±4.0 Hz of rated value.

[b]To within ±4.0 Hz of final value.

[c]To within ±5.0 percent of rated value.

[d]To within ±5.0 percent of final value.

[e]Refers to rated turbine conditions.

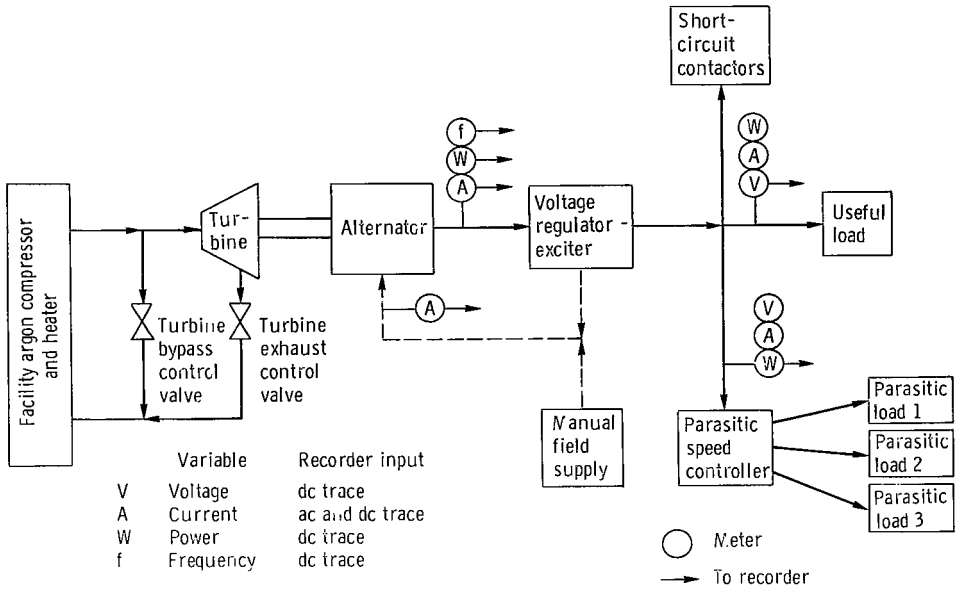

Figure 1. - Block diagram of test setup.

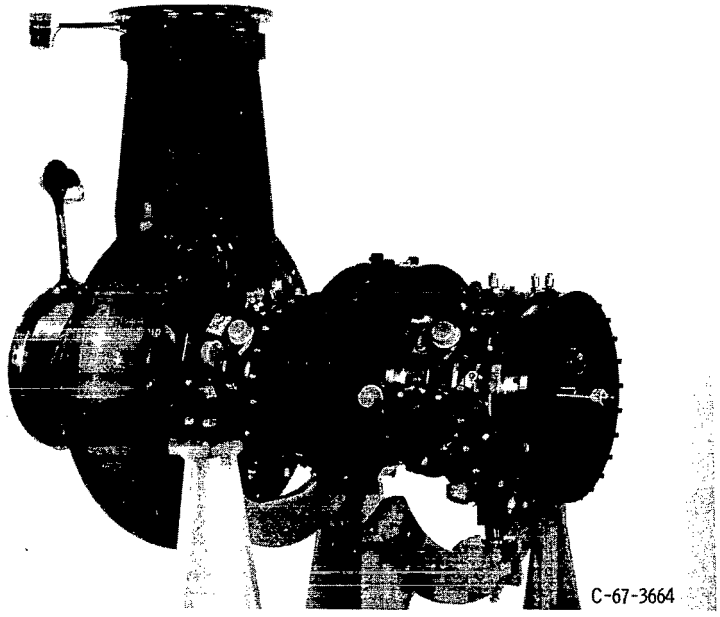

Figure 2. - Turboalternator.

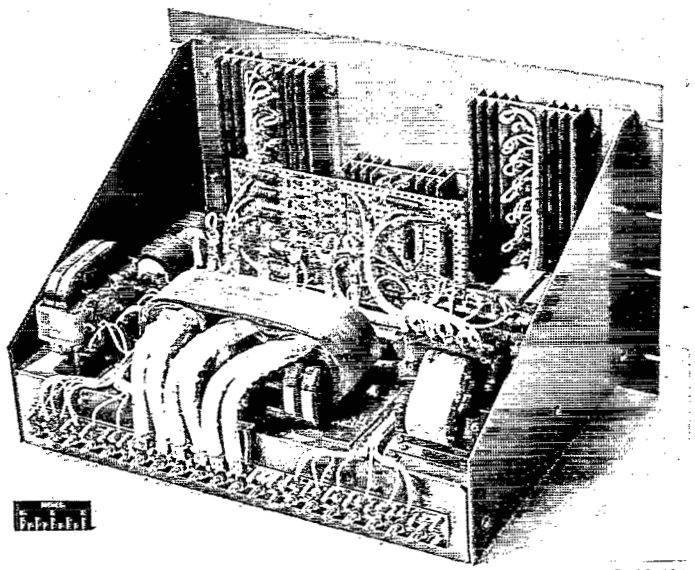

C-66-830

Figure 3. - Voltage regulator - exciter.

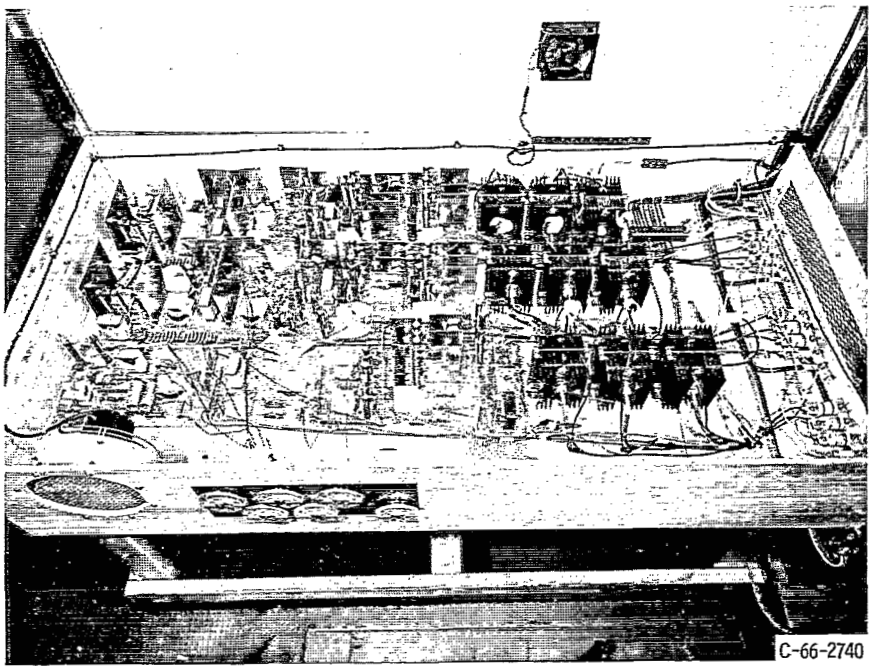

C-66-2740

Figure 4. - Parasitic-loading speed controller.

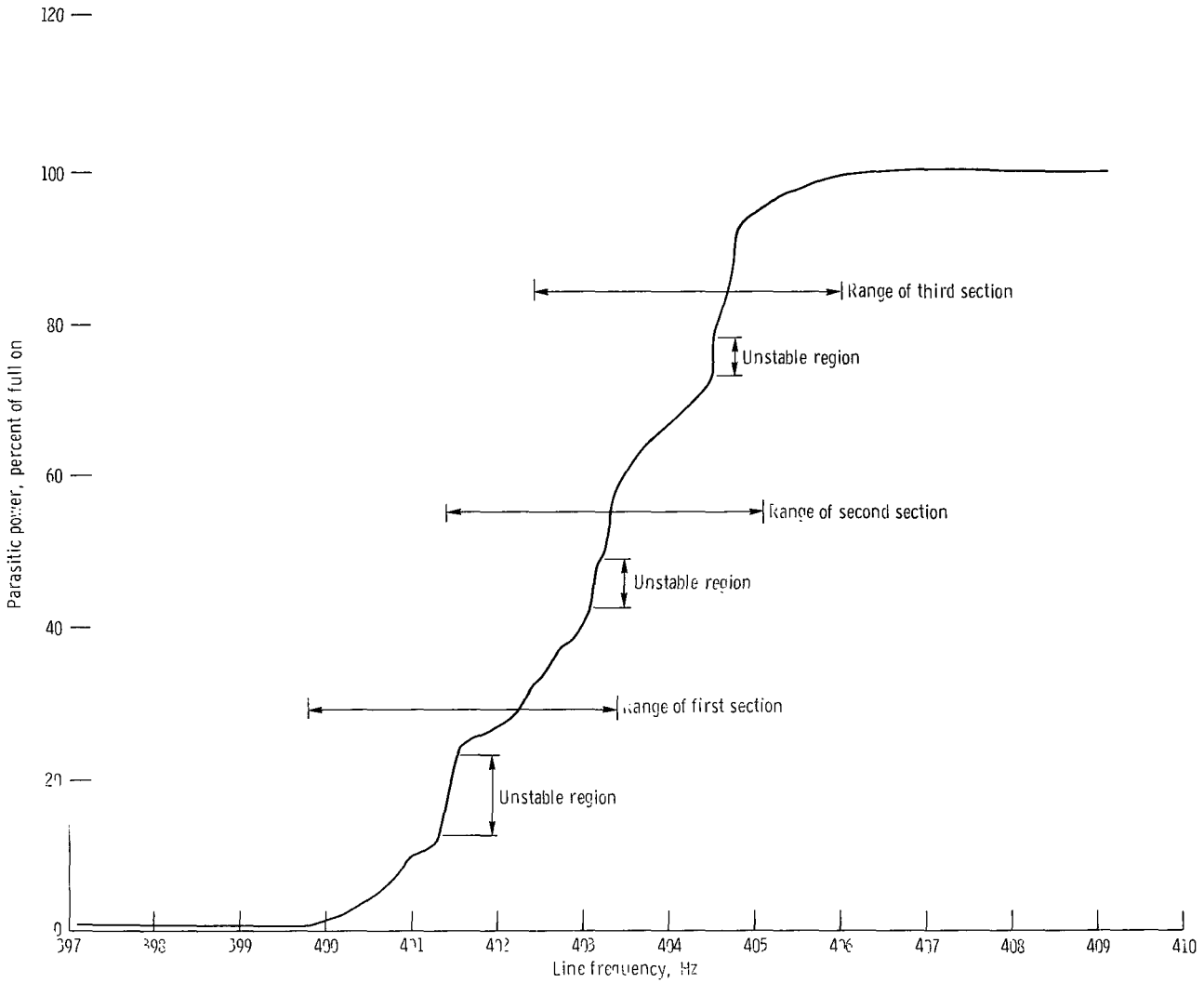

Figure 5. - Variation of parasitic power with frequency (before retuning).

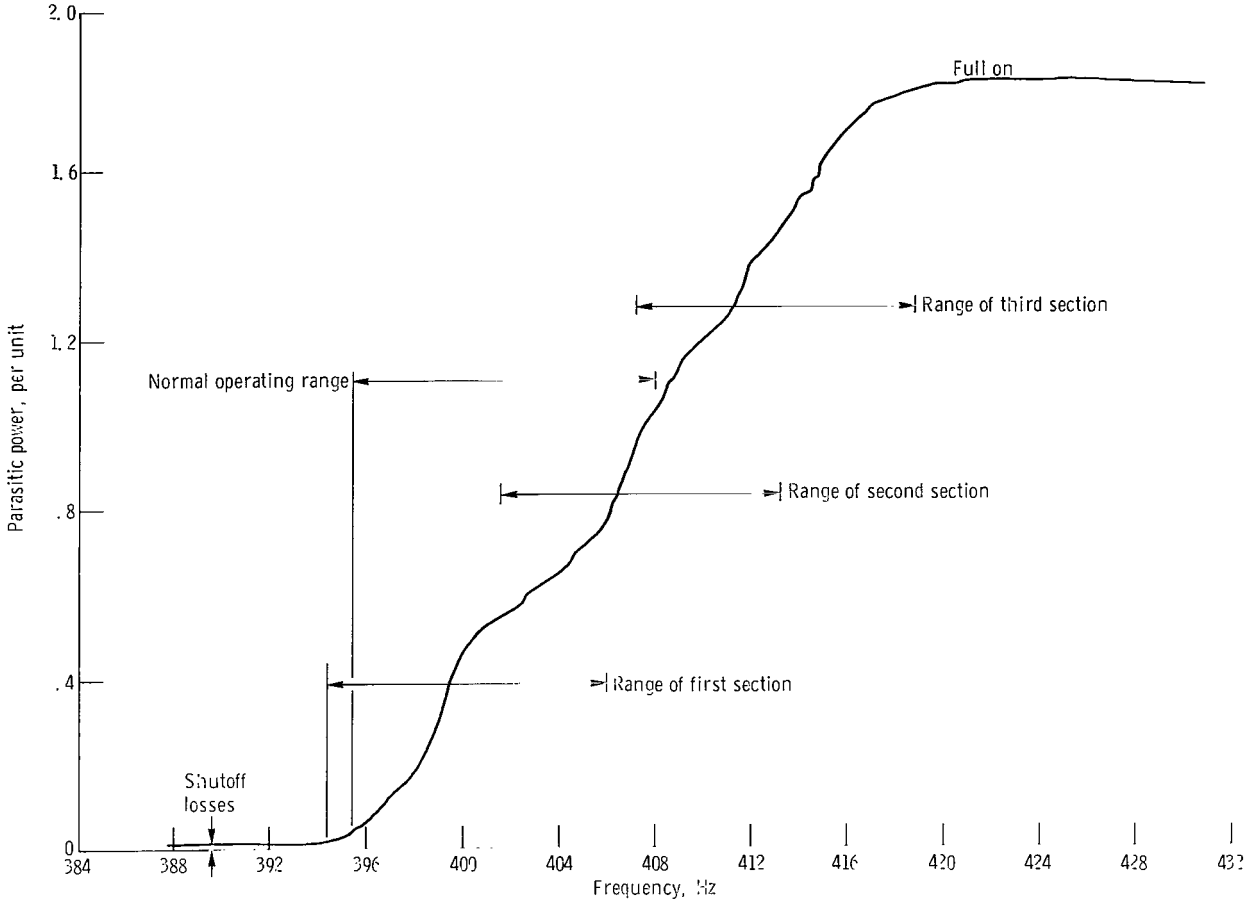

Figure 6. - Variation of parasitic power with frequency (after retuning). One per unit power = 9 kilowatts.

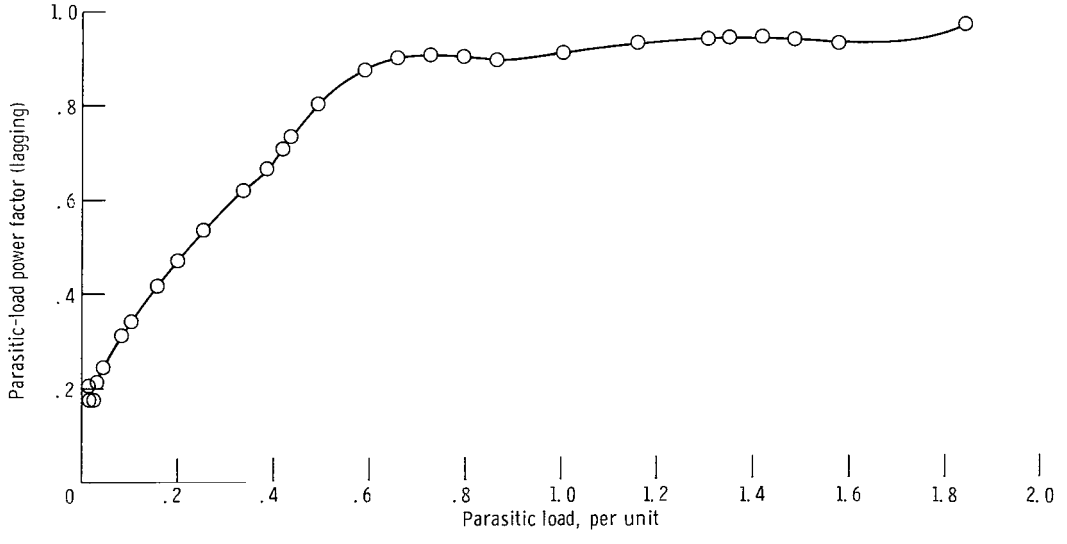

Figure 7. - Variation of parasitic-load power factor with parasitic load. One per unit power = 9 kilowatts.

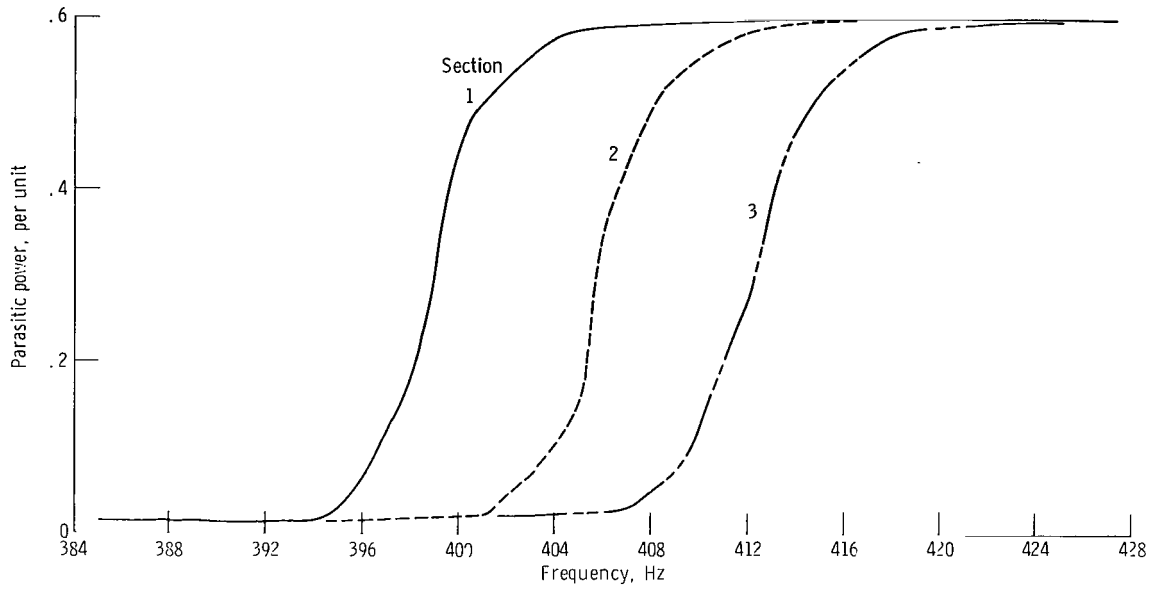

Figure 8. - Variation of parasitic power with frequency for each speed-control section. One per unit power = 9 kilowatts.

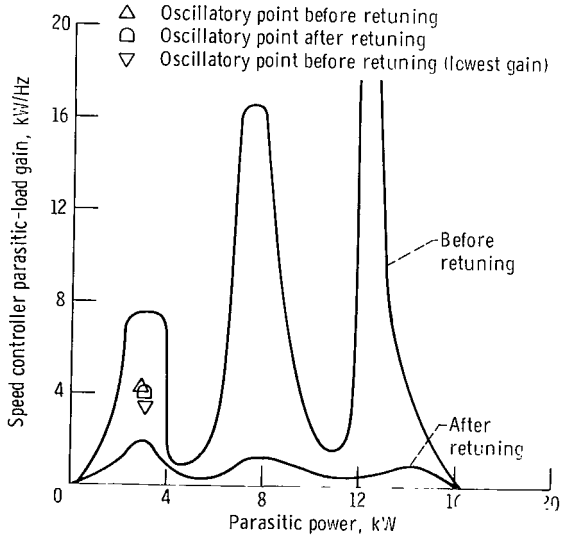

Figure 9. - Speed controller parasitic-load-gain variation with parasitic power.

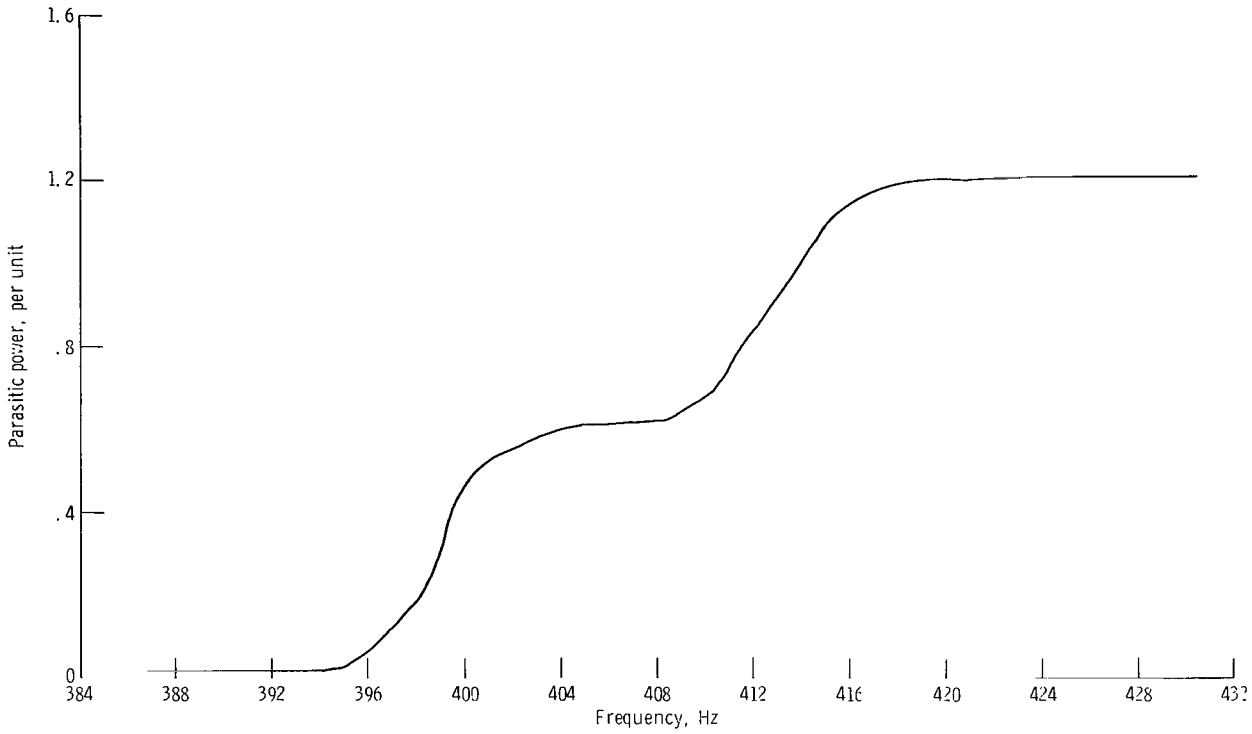

Figure 10. - Variation of parasitic power with frequency, with second section off. One per unit power = 9 kilowatts.

160
140
120
100
B
C
4
3
2
1
0
B
D
F
6
5
4
3
2
1
0
A
B
D
E
G

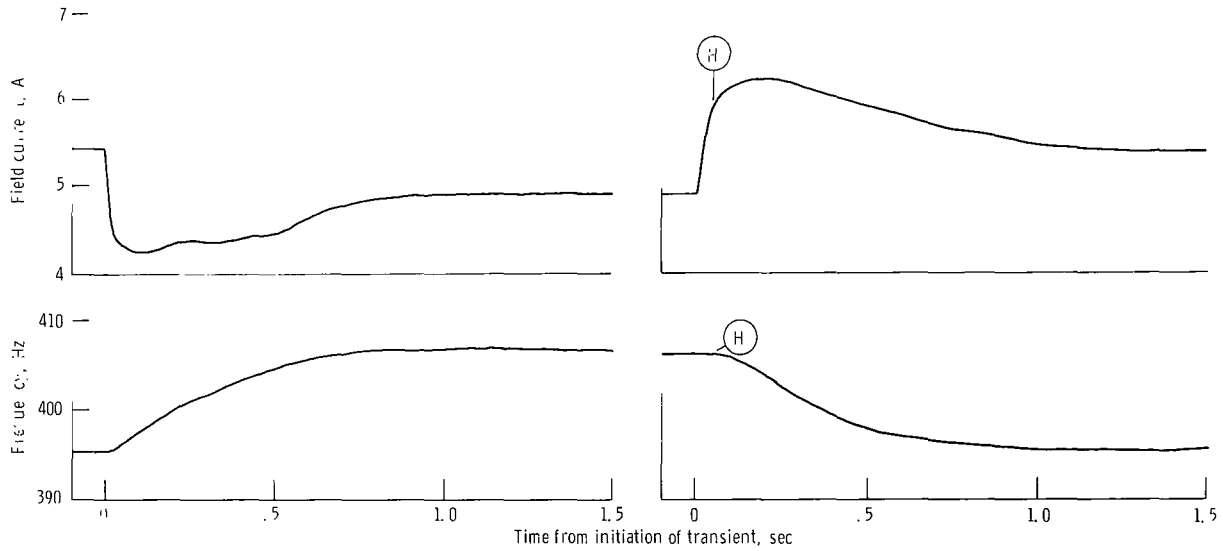

(a) Load stepped off.

(b) Load stepped on.

Figure 11. - Rated-load step transient (9-kilowatt, 0.8-power-factor (lagging) useful load stepped off and on).

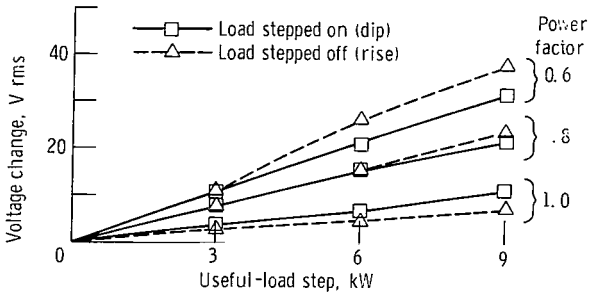

Figure 12. - Voltage-rise-and-dip variation with useful-load steps.

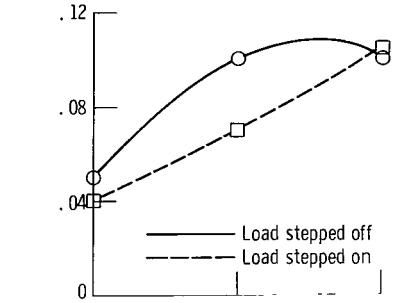

(a) Effect of 0.8-lagging-power-factor useful-load steps on electrical system voltage recovery time.

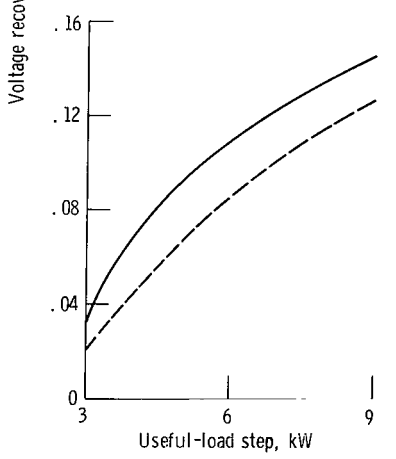

(b) Effect of 0.8-lagging-power-factor load steps on alternator and voltage regulator - exciter voltage recovery time. (Data from ref. 4.)

Figure 13. - Voltage-recovery-time characteristics.

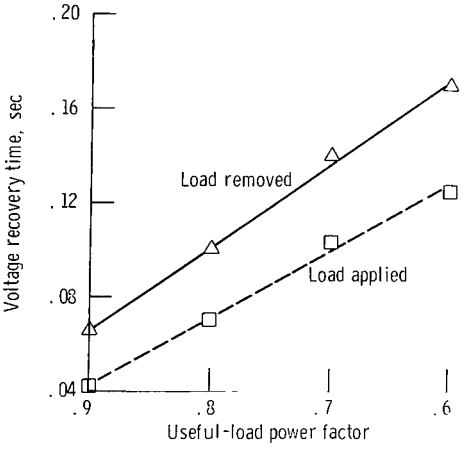

Figure 14. - Variation of voltage recovery time with useful-load power factor. Useful load, 6 kilowatts.

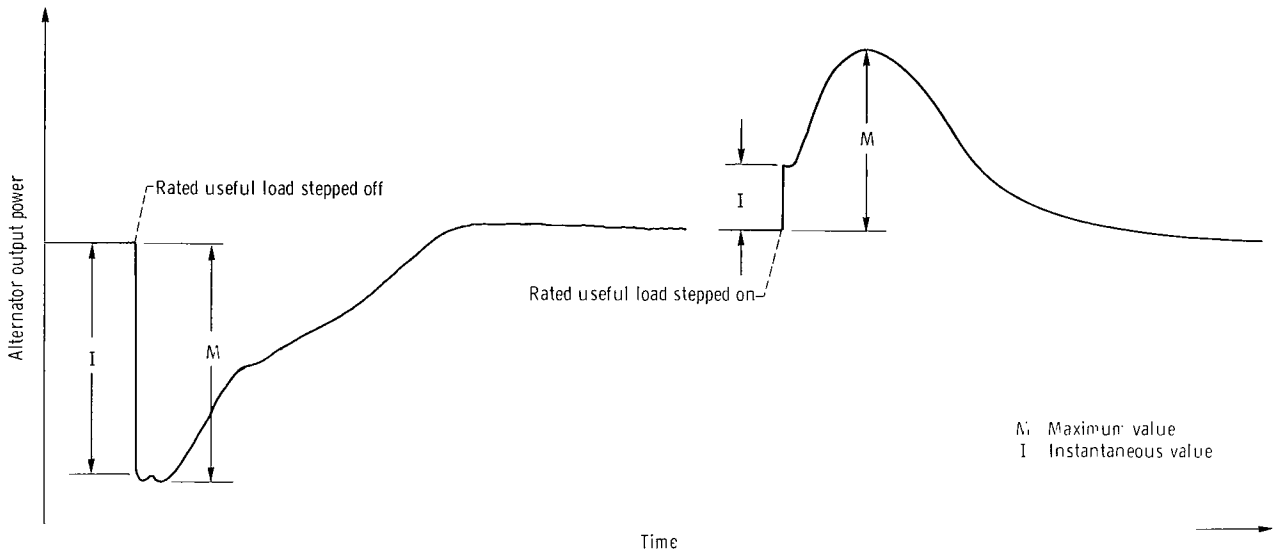

Figure 15. - Alternator output power fluctuation for a rated-useful-load step.

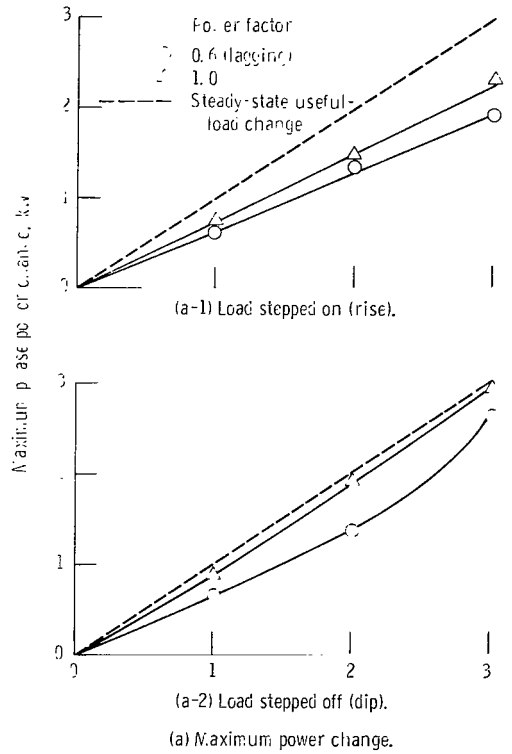

(a-1) Load stepped on (rise).

(a-2) Load stepped off (dip).

(a) Maximum power change.

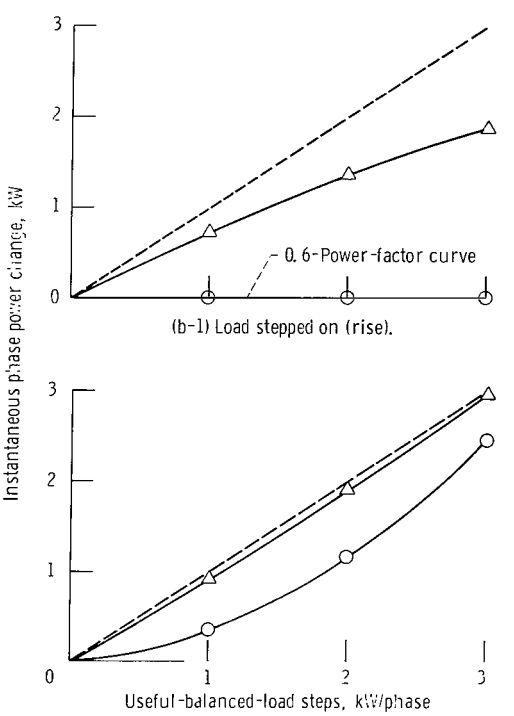

(b-1) Load stepped on (rise).

(b-2) Load stepped off (dip).

(b) Instantaneous power change.

Figure 16. - Turboalternator power-rise-and-dip variation with useful-load steps.

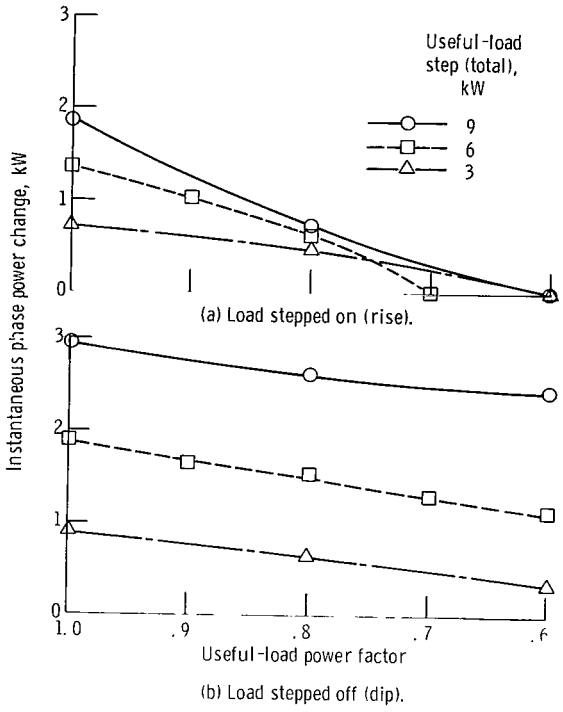

Figure 17. - Instantaneous turboalternator power-rise-and-dip variation with useful-load power factor.

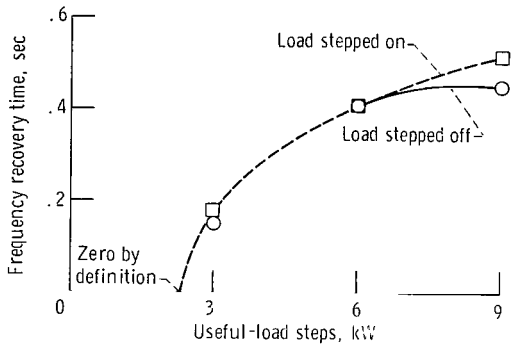

Figure 18. - Variation of frequency recovery time with useful-load steps. Recovery time is the time for the frequency to reach within 2 hertz of final value; 0.8-power-factor (lagging) useful load.

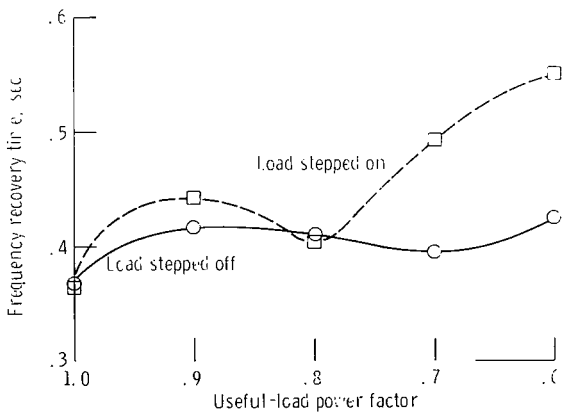

Figure 19. - Variation of frequency recovery time with 6-kilowatt useful-load power factor. Recovery time is the time for the frequency to reach within 2 hertz of final value.

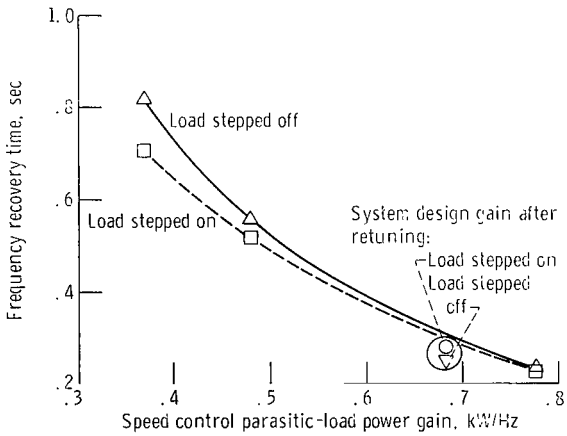

Figure 20. - Frequency-recovery-time variation with speed control parasitic-load power gain. Useful load, 6 kilowatts at 0.8 power factor. Recovery time is time for frequency to reach within 4 hertz of final value.

12x10^3
10
8
6
4
2
0
Speed, rpm
140
120
100
80
60
40
20
0
Useful-load voltage (L - N), V rms

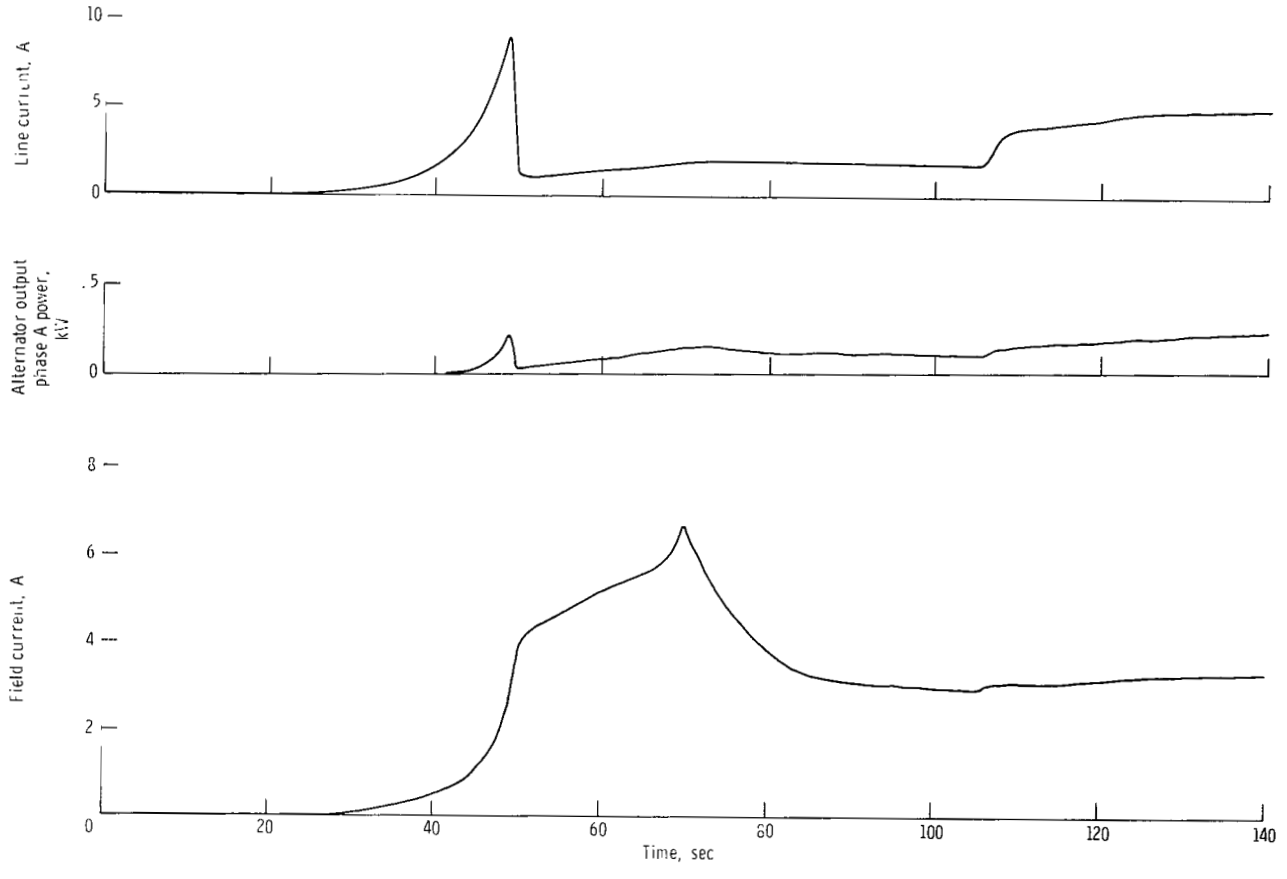

Figure 21. - Normal startup.

Speed, rpm
12×10^3
10
8
6
4
2
0

Useful-load voltage, V rms
140
120
100
80
60
40
20
0

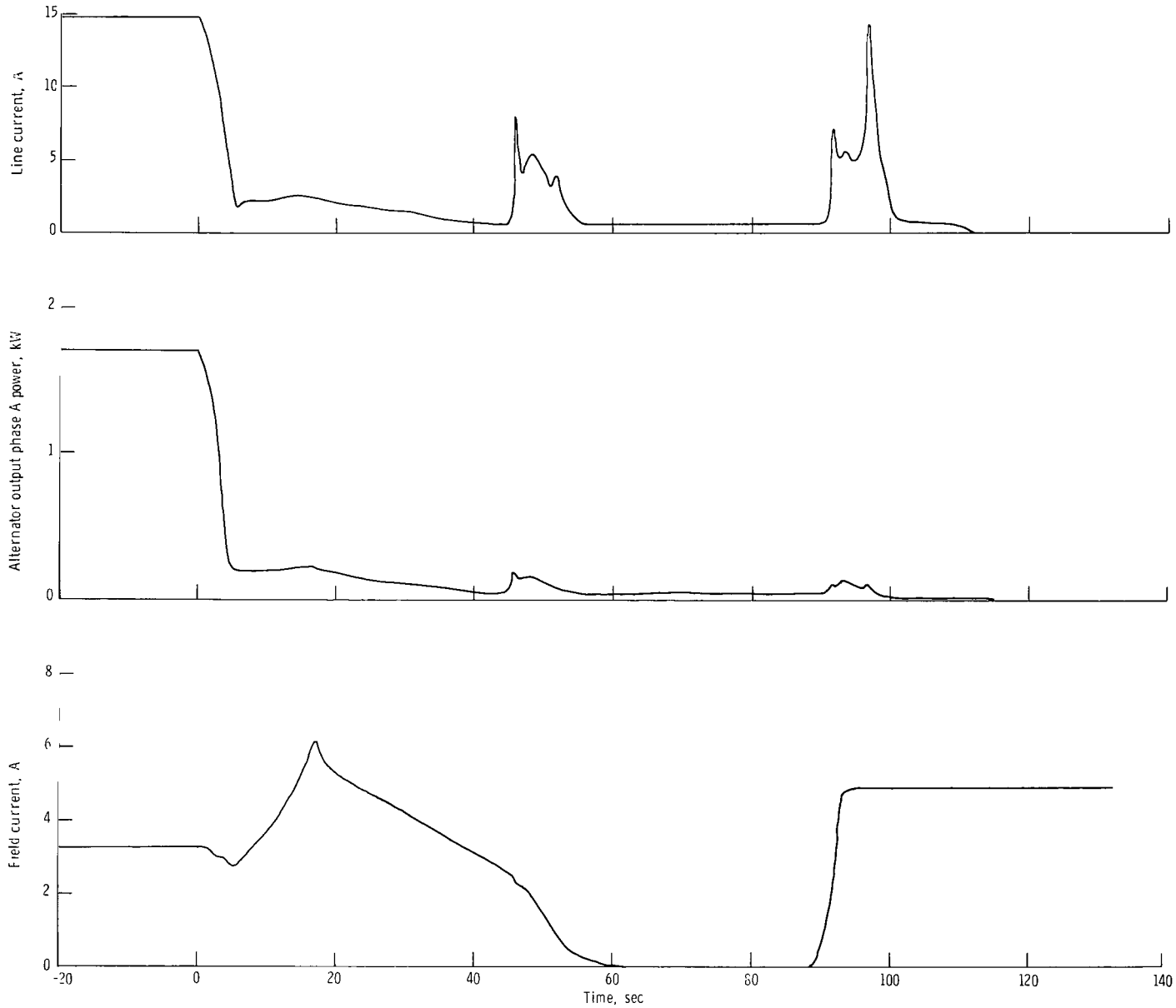

Figure 22. - Normal shutdown.

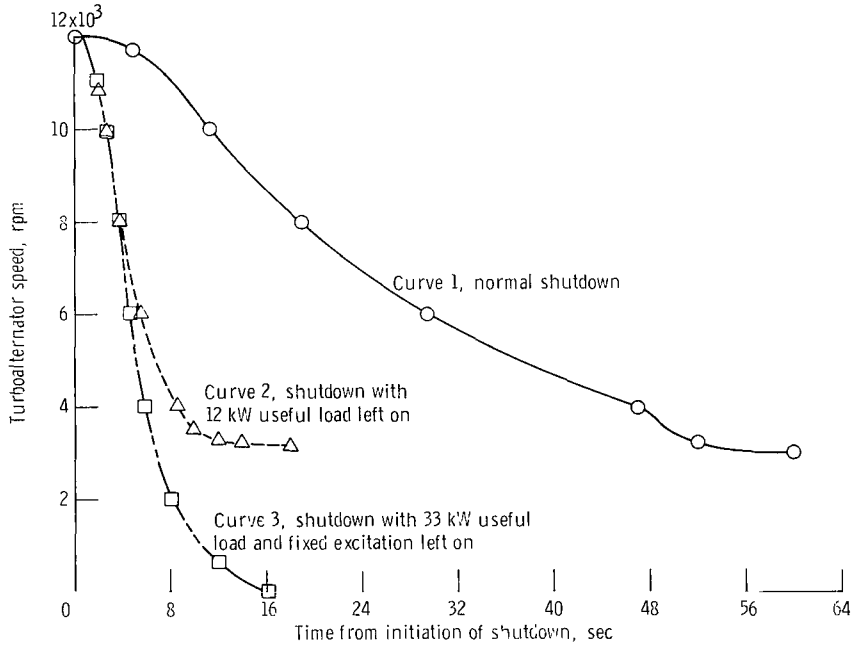

Figure 23. - Turboalternator speed variation with time during various shutdowns.

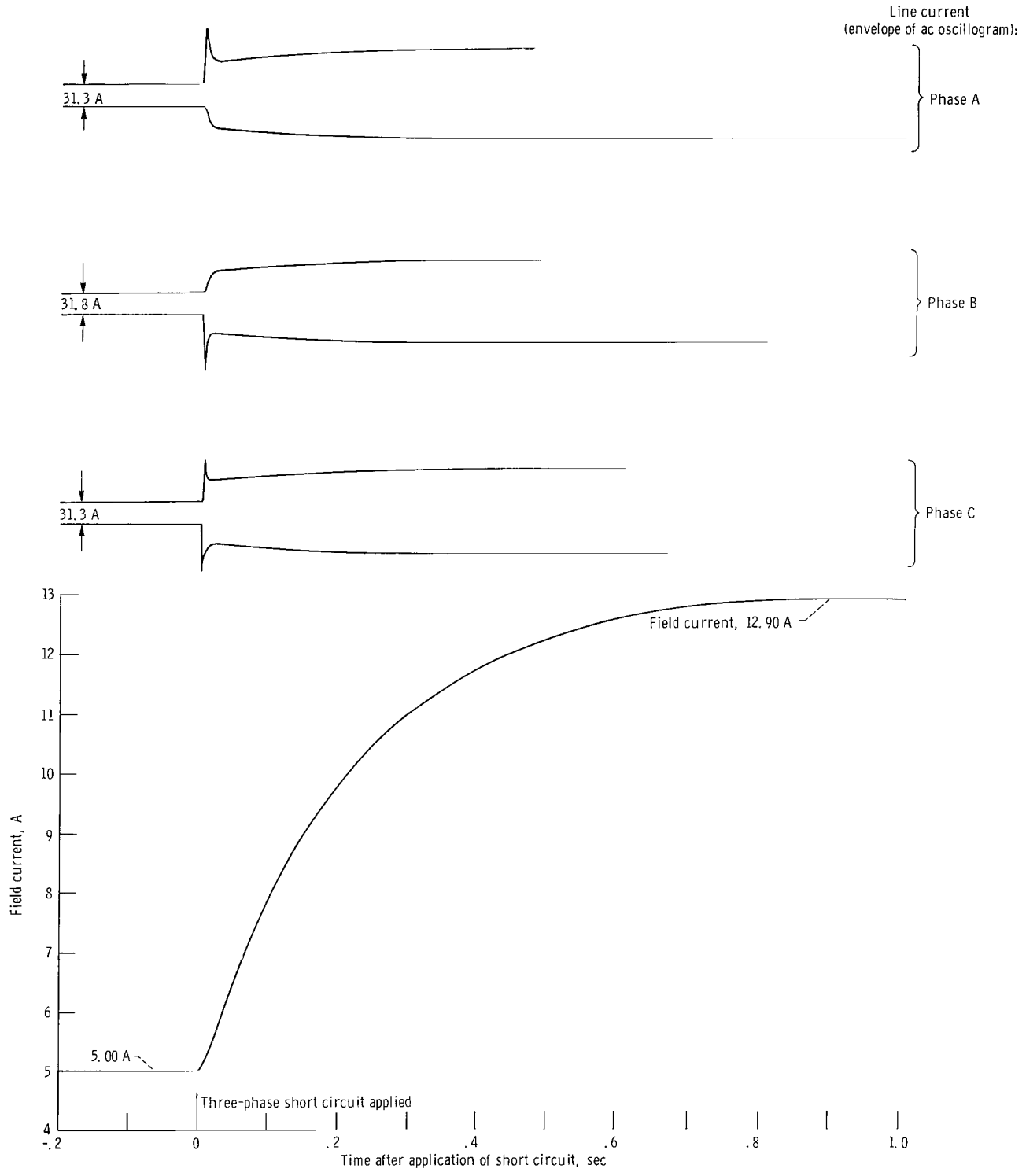

Figure 24. - Three-

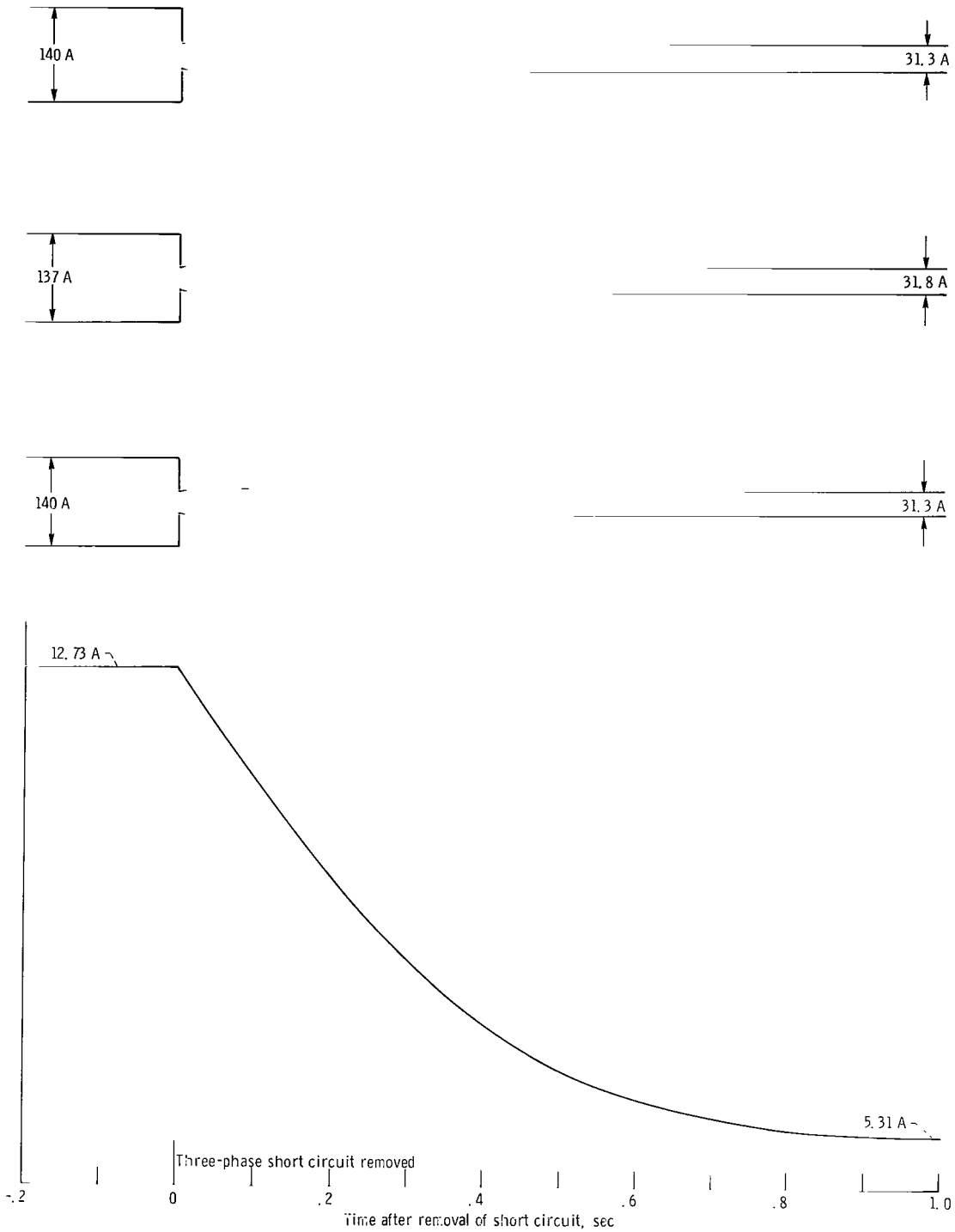

phase short circuit.

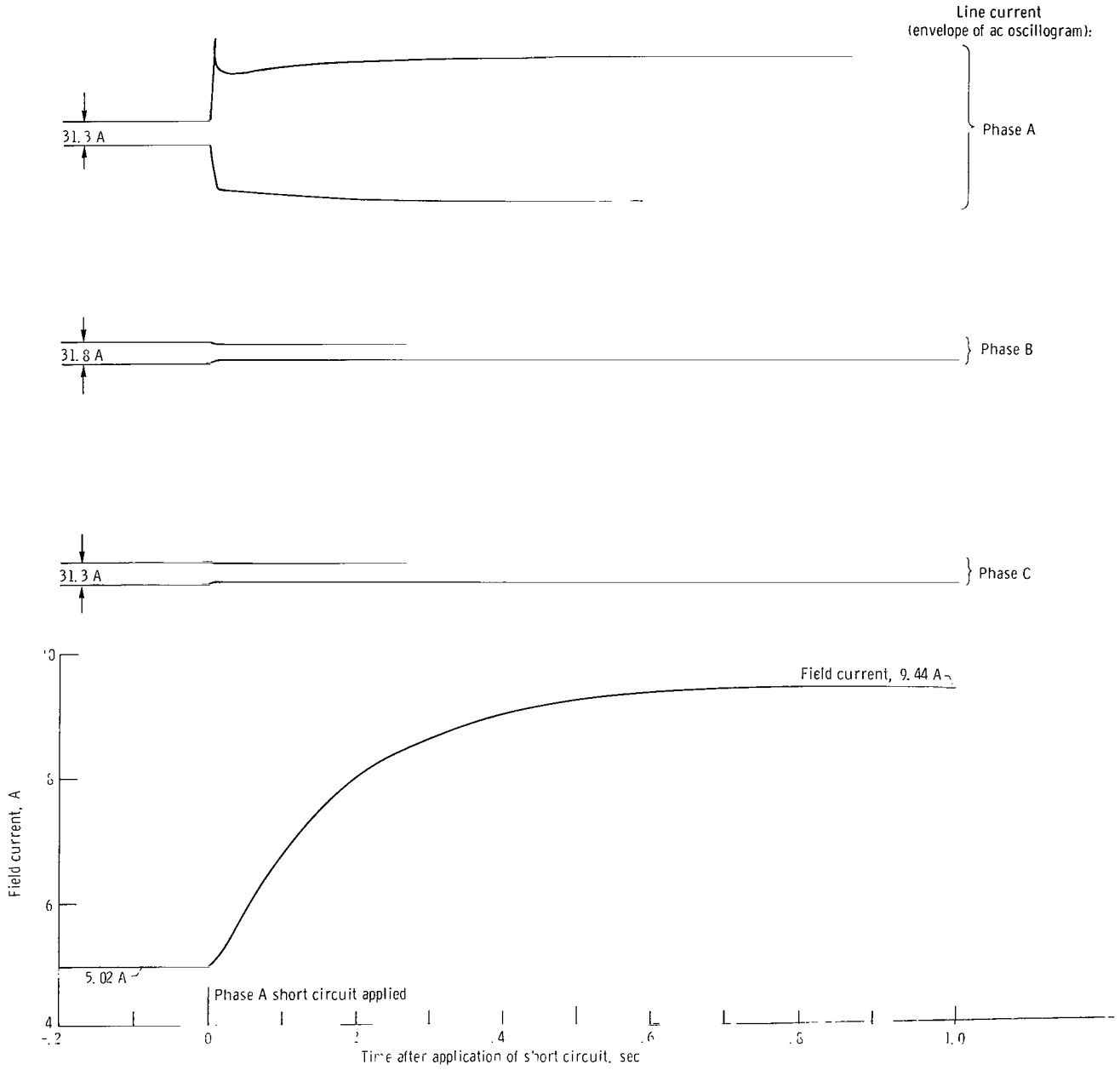

Figure 25. - Single-

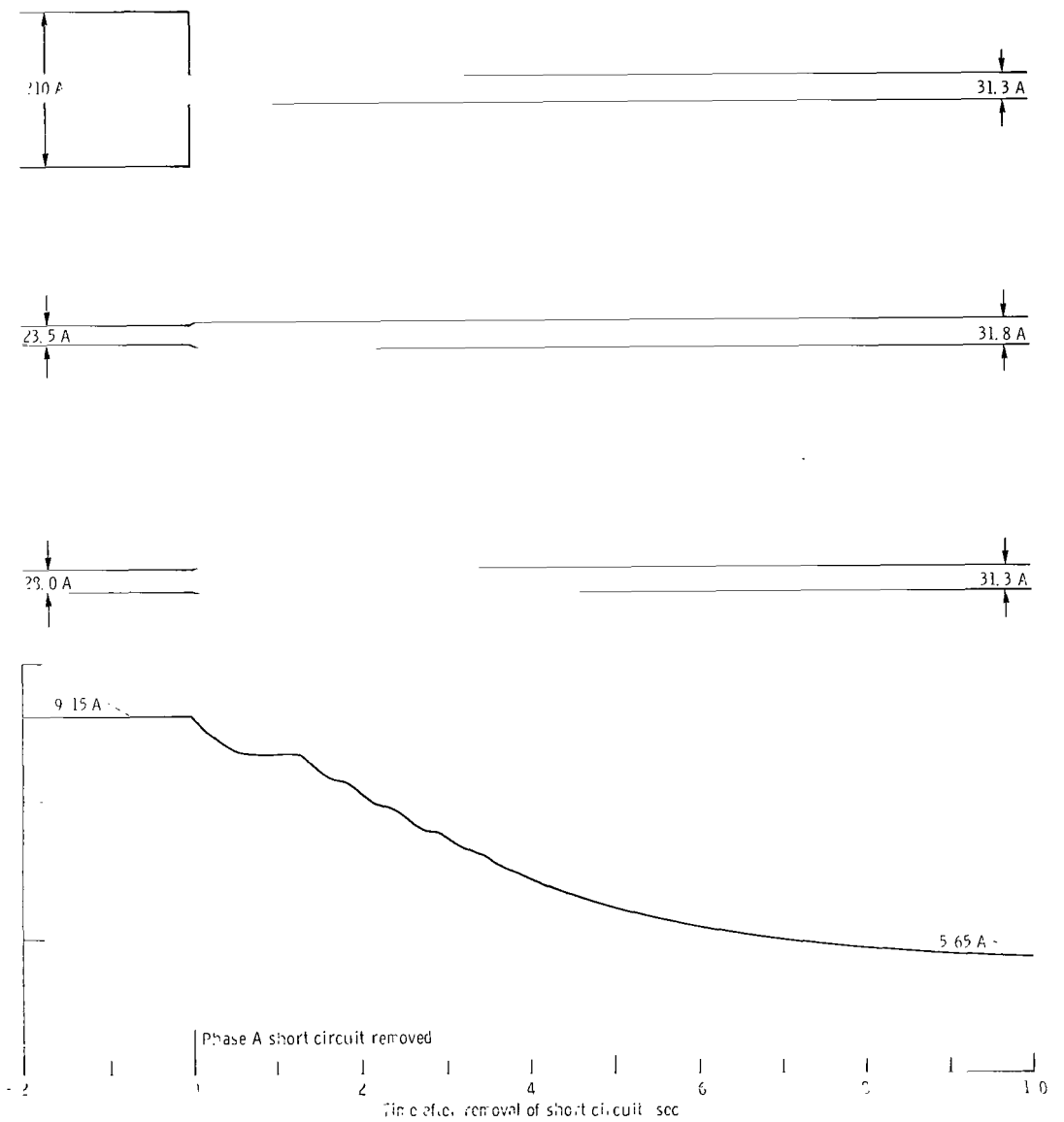

phase short circuit

01U 001 28 51 3DS 71088 00903
AIR FORCE WEAPONS LABORATORY /WLOL/
KIRTLAND AFB, NEW MEXICO 87117

ATT E. LOU BOWMAN, CHIEF, TECH. LIBRARY

"The aeronautical and space activities of the United States shall be conducted so as to contribute . . . to the expansion of human knowledge of phenomena in the atmosphere and space. The Administration shall provide for the widest practicable and appropriate dissemination of information concerning its activities and the results thereof."

—NATIONAL AERONAUTICS AND SPACE ACT OF 1958

NASA SCIENTIFIC AND TECHNICAL PUBLICATIONS

TECHNICAL REPORTS: Scientific and technical information considered important, complete, and a lasting contribution to existing knowledge.

TECHNICAL NOTES: Information less broad in scope but nevertheless of importance as a contribution to existing knowledge.

TECHNICAL MEMORANDUMS: Information receiving limited distribution because of preliminary data, security classification, or other reasons.

CONTRACTOR REPORTS: Scientific and technical information generated under a NASA contract or grant and considered an important contribution to existing knowledge.

TECHNICAL TRANSLATIONS: Information published in a foreign language considered to merit NASA distribution in English.

SPECIAL PUBLICATIONS: Information derived from or of value to NASA activities. Publications include conference proceedings, monographs, data compilations, handbooks, sourcebooks, and special bibliographies.

TECHNOLOGY UTILIZATION PUBLICATIONS: Information on technology used by NASA that may be of particular interest in commercial and other non-aerospace applications. Publications include Tech Briefs, Technology Utilization Reports and Technology Surveys.

Details on the availability of these publications may be obtained from:

SCIENTIFIC AND TECHNICAL INFORMATION OFFICE

NATIONAL AERONAUTICS AND SPACE ADMINISTRATION

Washington, D.C. 20546